DERIVATION AND APPLICATION OF A MULTI-PARAMETER GAMMA MODEL FOR ANALYZING THE RESIDENCE TIME DISTRIBUTION FUNCTION FOR NON-IDEAL FLOW SYSTEMS AS AN ALTERNATIVE TO THE ADVECTION DISPERSION EQUATION

A PROJECT REPORT

SUBMITTED TO THE COLLEGE OF ENGINEERING

IN

PARTIAL FULFILLMENT OF THE REQUIREMENTS

FOR THE DEGREE

OF

MASTER OF ENGINEERING

WITH A CONCENTRATION

IN

ENVIRONMENTAL ENGINEERING

IRUCKA AJANI EMBRY, E.I.T.
AUGUST 2012

August 2012

To the Dean of the College of Engineering:

We are submitting a project report by Irucka Ajani Embry entitled, “Derivation and Application of a Multi-Parameter Gamma Model for Analyzing the Residence Time Distribution Function for Non-Ideal Flow Systems as an alternative to the Advection Dispersion Equation.” We recommend that this be accepted in partial fulfillment of the requirement for the degree of Master of Engineering with a Concentration in Environmental Engineering.

_____
Committee Chair Date

_____
Committee Member
Date

_____
Committee Member
Date

_____
Department Head Date

_____
Associate Dean and Head of the
Date
Graduate Program

Accepted for the College of Engineering:

_____
Dean of the College of Engineering Date

COPYRIGHT PAGE

Derivation and Application of a Multi-Parameter Gamma Model for Analyzing the Residence Time Distribution Function for Non-Ideal Flow Systems as an alternative to the Advection Dispersion Equation

by

Irucka Ajani Embry

ABSTRACT

DERIVATION AND APPLICATION OF A MULTI-PARAMETER GAMMA MODEL FOR ANALYZING THE RESIDENCE TIME DISTRIBUTION FUNCTION FOR NON-IDEAL FLOW SYSTEMS AS AN ALTERNATIVE TO THE ADVECTION DISPERSION EQUATION

Irucka Embry, Graduate Student
Department of Civil and Environmental Engineering

A karst aquifer is modeled as a non-ideal flow system. Due to the complexity of possible flow paths in karst aquifers, it is difficult to create a mathematical framework to model the flow of contaminants and other particles through the aquifer. This project focuses on the mathematical development and application of a new residence time distribution (RTD) function for quantitative dye studies as an alternative to the traditional advection dispersion equation (ADE). This new method is based on a jointly combined four parameter gamma probability density function (PDF). The gamma residence time distribution (RTD) function and its first and second moments are derived from the individual two parameter gamma distributions of the randomly distributed variables tracer travel distance and linear velocity which is based on their relationship with time. **The purpose of this project was to compare the gamma RTD model, after being validated with laboratory data, to the ADE RTD model for a quantitative field tracer study performed at Mammoth Cave National Park.** Generally, a

tracer study is performed to qualitatively or quantitatively approximate the flow conditions. The quantitative results of the tracer experiment are displayed in the tracer breakthrough curve which represents the effluent tracer concentration over time. The breakthrough curve can be used to determine the residence time distribution (RTD) function. The RTD function numerically describes the time that particles have spent reacting in a system. The normalized forms of the gamma RTD and the advection dispersion equation RTD were compared with the normalized tracer RTD. The normalized gamma RTD function had a lower mean-absolute deviation (MAD) than the normalized advection dispersion equation when compared to the normalized tracer RTD function. The gamma RTD function is tied back to the actual physical site due to its randomly distributed variables. This verification suggests that the gamma RTD function is a suitable alternative to the advection dispersion equation RTD function for quantitative tracer studies of karst aquifers and other non-ideal flow systems.

DEDICATION

This Master Thesis is dedicated to everyone that has supported me in many ways over the course of my Life. You know who you are. Thank-you very much!

It is also dedicated to the previous students who have contributed to our understanding of karst aquifers, of non-ideal and ideal flow systems, and of the residence time distribution function based on the advection dispersion equation and the gamma distribution.

It is also dedicated to all the developers, programmers, advocates, etc. of Free/Libre and Open Source Software (FLOSS) that I have used throughout my entire Master degree program (and previously), including the completion of my Master Thesis.

IAE

ACKNOWLEDGMENTS

Financial & Research Support

In addition to the great support and encouragement that I have received from my advisors, I would like to thank the following for research and/or financial support over the past 2 years: United States Department of Education Title 3; United States Department of Energy (DOE) National Nuclear Security Administration (NNSA); United States Geological Survey {USGS} (Tennessee Water Science Center); Tennessee State University (TSU) College of Engineering & the Department of Civil and Environmental Engineering faculty & staff; Dr. Rick Toomey & Shannon Trimboli (Mammoth Cave International Center for Science and Learning, Kentucky); Bobby Carson, Steve Kovar, Eddie Wells, etc. (Mammoth Cave National Park System, Kentucky).

Student Assistance

I would like to thank the following students for assistance, encouragement, and/or meaningful discussions, etc. over the past 2 years: Victor Roland and my fellow Environmental Engineering laboratory mates & the previous students working on residence time distribution analysis.

Software Assistance

This Master's Thesis was written using free software and free software fonts (Liberation Serif, Liberation Sans, and Liberation Mono) on a free software distribution of GNU/Linux (Trisquel) using the free software X Window System desktops: K Desktop Environment (KDE) and the GNOME Desktop Environment. It was typeset In LibreOffice Writer. JabRef was used for managing the bibliographic database.

I would like to acknowledge the Free/Libre and Open Source Software (FLOSS) that I have used over the past 2 years (and previously): Trisquel GNU/Linux {GNU/Linux Operating System distribution} (http://trisquel.info/); Mandriva Linux {GNU/Linux Operating System distribution} http://www.mandriva.com/; Mageia {GNU/Linux Operating System distribution} (http://www.mageia.org/); KDE (K Desktop Environment) {X Window System desktop}(http://www.kde.org/); GNOME {X Window System desktop} (http://www.gnome.org/); Liberation Font family (https://fedorahosted.org/liberation-fonts/); GNU FreeFont family (http://www.gnu.org/software/freefont/); GNU Octave (http://www.octave.org); Octave-Forge (http://octave.sourceforge.net/); gnuplot (http://www.gnuplot.info); FLTK (http://www.fltk.org/index.php); LibreOffice Suite (http://www.libreoffice.org); LibreOffice Extensions (http://extensions.libreoffice.org/); OpenOffice.org {now Apache OpenOffice}

(http://www.openoffice.org/); Repository for (Apache) OpenOffice Extensions (http://extensions.services.openoffice.org/); Sage (http://www.sagemath.org/); GIMP {GNU Image Manipulation Program} (http://www.gimp.org); Scribus (http://www.scribus.net/canvas/Scribus); LyX (http://www.lyx.org); TeX (http://www.tug.org); LaTeX (http://www.latex-project.org); Inkscape (http://inkscape.org/); JabRef (http://jabref.sourceforge.net); Kate (http://kate-editor.org/); gedit (http://projects.gnome.org/gedit/); Filezilla (http://filezilla-project.org/); Notepad++ (http://www.notepadplusplus.org/); Crimson Editor (http://www.crimsoneditor.com/); Mozilla Firefox (http://www.mozilla.org/firefox); Firefox Add-ons (https://addons.mozilla.org); Kalzium – Periodic Table of Elements (http://www.kde.org/applications/education/kalzium/); QCAD Community Edition (http://www.ribbonsoft.com/en/qcad); Qalculate! (http://qalculate.sourceforge.net/); ODEToolkit (http://odetoolkit.hmc.edu/index.html); Tellico (http://tellico-project.org/); etc.

IAE

Table of Contents

COPYRIGHT PAGE....4
ABSTRACT....5
DEDICATION....7
ACKNOWLEDGMENTS....8
LIST OF FIGURES....12
LIST OF TABLES....14
NOMENCLATURE....15
CHAPTER 1....1
CHAPTER 2....11
CHAPTER 3....22
CHAPTER 4....33
CHAPTER 5....42
REFERENCES....46
APPENDICES....55
APPENDIX A....56
APPENDIX B....66

LIST OF FIGURES

FIGURE	DESCRIPTION	PAGE
1.1	United States Geological Survey (USGS) Karst Interest Group (KIG) Karst Map displayed on their Web site, each karst aquifer is denoted by a different color pattern on the map.	6
1.2	United States Geological Survey (USGS) and National Cave and Karst Research Institute (NCKRI) Preliminary National Karst Map, this map shows potential karst areas in the continental United States over geologic domains where the blue, green, and purple areas constitute carbonate rocks and the orange areas are evaporite rocks.	7
3.1	Diagram displays the types of flow possible in karst aquifers, from diffuse flow through mixed, to conduit flow. This research was done at Mammoth Cave, Kentucky, which is considered a mix of diffuse and conduit flow, perhaps more conduit than diffuse.	22
3.2	Topographic map of cave features with surface overlay. The green line represents the surface stream and a probable flow path of the dye to both Shaler's Brook and Devil's Cooling Tub. The red, blue, and purple lines delineate cave passages. (Courtesy of Dr. Rick Toomey at the Mammoth Cave International Center for Science and Learning)	25
3.3	1908 Tour Map showing the 200 ft level of the cave showing cave features by their colloquial names, which are used to this day. Annette's Dome (Annetta's Dome on the map) and Devil's Cooling Tub were referred to in this study. {Courtesy of Dr. Rick Toomey at the Mammoth Cave International Center for Science and Learning}	27
3.4	Photograph showing the dye and salt release mechanism. Also shown in the picture are the 1st flush sampler and the YSI datasonde	30
3.5	Photograph showing the pool at the bottom of Annette's Dome and the beginning of Shaler's Brook. Also pictured is the YSI datasonde (gray and yellow tube in water) and the 1st flush sampler (white gallon jar).	31

3.6	Picture showing the GGUN-FL Fluorometer 80526 next to the YSI datasonde in Devil's Cooling Tub on December 20, 2011.	32
4.1	Tracer concentration versus time for the dye study at Shaler's Brook. This data was used to determine the mean, variance, and Péclet number for the karst system.	36
4.2	Tracer concentration versus time for the dye study at Devil's Cooling Tub.	37
4.3	Tracer concentration versus time for the dye study at Devil's Cooling Tub. This figure provides a better view of the first peak.	38
4.4	Tracer concentration versus time for the dye study at Devil's Cooling Tub. This figure provides a better view of the second peak.	39
4.5	Comparing the normalized forms of the advection dispersion equation RTD and the gamma RTD models to the normalized tracer RTD model for the field tracer study at Shaler's Brook.	40

LIST OF TABLES

TABLE	DESCRIPTION	PAGE
3.1	Elevation and Distance Estimates for the Site Area	24
A.1	Raw YSI datasonde data for Shaler's Brook	56
A.2	Raw GGUN-FL Fluorometer 80526 data for Devil's Cooling Tub (1st Hit)	58
A.3	Raw GGUN-FL Fluorometer 80526 data for Devil's Cooling Tub (2nd Hit)	62

NOMENCLATURE

L	travel distance
v	velocity
t or T	time
t_m	mean residence time
σ^2	distribution variance
θ	dimensionless time
C(t)	concentration over time
C_T	concentration at time t
C_{T0}	concentration at time t = 0
V	reactor or system volume
V_{eq}	equivalent volume
A_{eq}	equivalent area
eq	equivalent
Q	volumetric flow rate
τ	space time
irv	independent random variable
RTD	residence time or residence-time distribution
E(t)	residence time or residence-time distribution function
TTD	transit time distribution
DTD	detention time distribution
HRTD	hydraulic residence time distribution
ADE	advection dispersion equation
AxDE	axial dispersion equation
ADM	axial dispersion model
CDE	convection dispersion equation
PDF	probability density function
PFR	plug-flow reactor
CFSTR	continuous-flow stirred tank reactor
CSTR	continuous-stirred tank reactor
Pe	Péclet number
MAD	mean-absolute deviation
DEPS	Differential Evolution & Particle Swarm Optimization algorithm

CHAPTER 1

INTRODUCTION

1.1 Residence Time Distribution

Researchers have used the distribution of residence times to examine the characteristics of a non-ideal flow reactor or system. The distribution of residence times or the residence time distribution (RTD) was first proposed to analyze chemical reactor performance in a paper by MacMullin and Weber in 1935 [1, 2, 3]. It was not until after Danckwerts' publication of "Continuous Flow Systems. Distribution of Residence Times," in 1953, that the RTD theory was organized in a more structured manner and most of the distributions were classified [2-5]. Many people still use Danckwerts' work as their foundation for analysis of systems with the RTD model. The residence time distribution of a system characterizes the mixing that happens in a system and the quantity *E(t)* is the residence time distribution function. This function describes quantitatively the amount of time that different fluid particles have spent in the system. *E(t)* is also a probability density function (PDF) that defines the probability that a particle entering the system will remain there for a time *t* (see [1-8] for a thorough explanation of the background theory to mixing and RTD).

A non-ideal flow system can be modeled as a chemical reactor as this work started in chemical engineering. The main types of reactors, referred to in the literature, are: 1) the batch reactor; 2) the complete-mix reactor which can also be called the continuous-flow

stirred tank reactor (CFSTR), continuous-stirred tank reactor (CSTR), or backmix reactor in chemical engineering literature; 3) the plug-flow reactor (PFR) also referred to as the tubular-flow reactor or plug-flow tubular reactor; 4) complete-mix reactors in series; 5) the packed-bed reactor; and lastly 6) the fluidized-bed reactor. Our research focuses on modeling non-ideal flow systems as a plug-flow reactor. The plug-flow reactor when modeled ideally has instantaneous and complete dispersion, but this is not the case in a non-ideal PFR. Non-ideal flow happens when some flow particles reach the outlet before the main portion reaches the same exit – that is assuming that all the particles entered the inflow at the same time [2-3, 7]. The important aspect of non-ideal flow, for the work that we concentrate on in our environmental engineering program with regards to bioremediation and karst aquifers, is that a part of the flow will not stay in the system long enough for biochemical reactions to go to completion.

In an ideal plug-flow reactor the fluid molecules move in the system with little or no axial or longitudinal mixing (or dispersion) and leave the reactor in the same sequence that they entered the system. It is important to note that in addition to the limited role of axial dispersion in an ideal PFR there can also be movement due to advection and dispersion. “Advection is the process of dissolved or colloidal particle movement with the flow velocity. Dispersion is the axial or longitudinal molecule movement which is caused by velocity differences, turbulent eddies, and molecular diffusion.” “In an ideal PFR the molecules are treated the same and are kept in the reactor for a time that is equal to the

theoretical detention time (volume V over the volumetric flow rate Q). This flow regime is best approximated in long open tanks where the longitudinal dispersion is either minimal or not present and with a high length-to-width ratio. Essentially all particles leaving the ideal PFR and batch reactor have been inside of it for the same length of time thus having the same residence time. The time that molecules have spent in the reactor or system is the residence time of the particles in the reactor. The various molecules in the system spend different times inside the reactor in the other reactor types, thus there is a particle distribution of residence times within the reactor. This distribution can affect the performance of any reactor. Many of the particles leave the system after spending a time close to the mean residence time. The residence time distribution (RTD) of a system can be defined by the mixing that occurs in the system. Axial mixing does not occur in a PFR and this is shown in the RTD curve produced by this type of reactor. The continuous-stirred tank reactor (CSTR) is thoroughly mixed and displays a different RTD curve than the plug-flow reactor. The RTD curve displayed by a given reactor provides information about the mixing that occurs within the system. Further analysis of the RTD curve provides information about the time that molecules spend in the system" [2-3, 7]. A karst aquifer is an example of a non-ideal flow system.

More specifically, the operation of a non-ideal flow chemical reactor is analogous to a contaminant release into a karst aquifer and the eventual discharge of this contaminant at a down gradient spring or other exit point [9]. What exactly is karst?

1.2 Karst Terrain

“Karst is a term used to describe a distinctive set of physical conditions, landforms, hydrology, and bedrock attributes that may be present in areas that are underlain by bedrock that are appreciably soluble in water, such as limestone, dolomite, and gypsum. Karst is a term used to denote areas that contain surface and subsurface features, such as fissures; tubes; cavern openings; caves; losing, sinking, gaining, and underground streams; springs; sinkholes; karst windows; and a unique hydrogeology that results in aquifers that are highly productive but extremely vulnerable to contamination. Nearly all surface karst features are formed by internal drainage, subsidence, and collapse caused by the development of underlying caves. In the United States, about 40% of the groundwater used for drinking comes from karst aquifers.” Other features of karst topography include “low density of surface water drainageways, closed depressions with internal drainage, groundwater levels that may vary appreciably over relatively short distances, thin soils, high flow rate springs, and hard groundwater and bicarbonate chemistry in streams.” [10-14]

“Karst hydrogeology is typified by a network of interconnected fissures, fractures and conduits emplaced in a relatively low-permeability rock. Most of the groundwater flow and transport occurs through the network of openings, while most of the groundwater storage occurs in the matrix. As a result, most karst aquifers are highly heterogeneous and anisotropic, and much of karst research has focused on developing innovative approaches for better understanding and managing these valuable water resources” [10].

“Karst terrain is present in 18% of the lower 48 states of the United States and 25% of the world. Rather than overland flow through streams, karst water flows below ground through systems of conduits and fractures until it emerges as a spring. Surface drainage through stream networks disappears, and sinkholes replace these features as the subsurface flow increases due to ever-enlarging conduits. Subsurface water in these systems moves very quickly to a spring, similar in speed to pipeflow. A myriad of local planning problems are specific to karst landscapes, including sinkhole collapse, sinkhole flooding, and an easily pollutable groundwater supply. In non-karst areas, groundwater moves far more slowly, and this laminar flow and contact with soil and soil organisms allows for greater removal of contaminants from groundwater than in karst regions” [13]. Figures 1.1 and 1.2 provide an overview of the karst terrain expected over the continental United States.

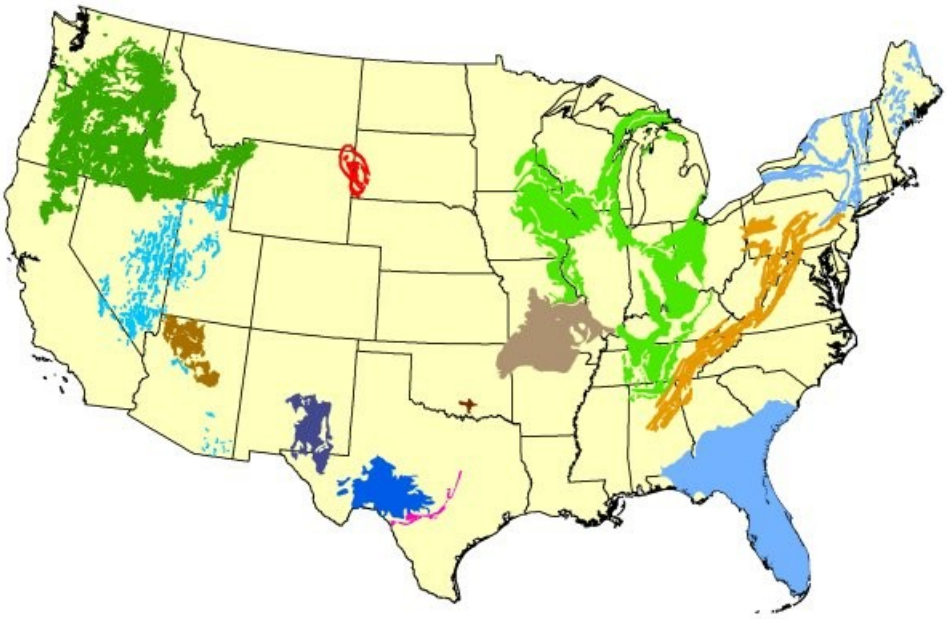

Figure 1.1 United States Geological Survey (USGS) Karst Interest Group (KIG) Karst Map displayed on their Web site, each karst aquifer is denoted by a different color pattern on the map [10].

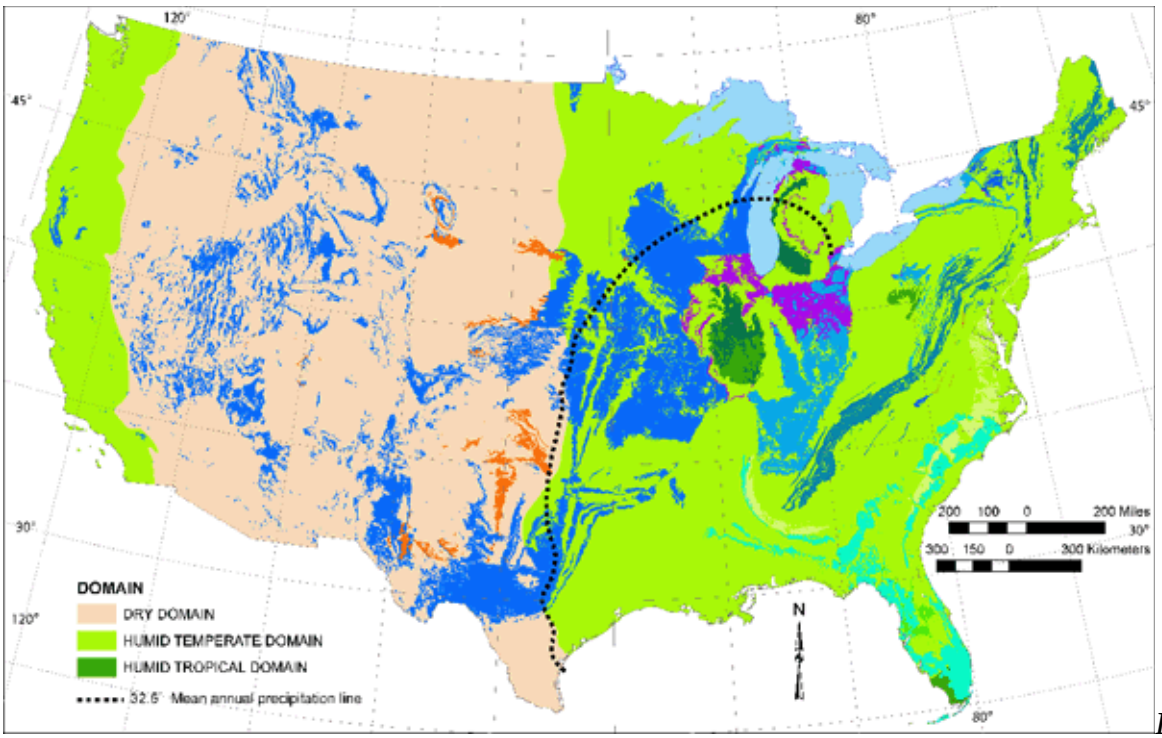

Figure 1.2 United States Geological Survey (USGS) and National Cave and Karst Research Institute (NCKRI) Preliminary National Karst Map, this map shows potential karst areas in the continental United States over geologic domains where the blue, green, and purple areas constitute carbonate rocks and the orange areas are evaporite rocks [15].

1.3 Why are Karst Aquifers so Important?

As aforementioned in section 1.2 and shown in Figures 1.1 and 1.2, approximately 18% of the United States' and 25% of the world's terrain are karstic in nature and about 40% of the United States drinking water supplies comes from groundwater in karst aquifers. The groundwater in karst aquifers like most other groundwater sources are subject to contamination, but karst aquifers are more susceptible. Karst aquifers, generally, have a more direct connection to surface activities and surface runoff and pollutants can quickly

travel to karst groundwater systems [14]. The karst aquifer can include subsurface conduit networks (pipelines) which occur with sinkholes and sinking streams. Also, the water and the solute (dissolved particles) in the water will flow through the karst aquifer into the groundwater system without natural filtering or sorption (sticking) of the solute to soil particles [16]. Due to the sinking streams, sinkholes, and other karst features, it is hard to investigate karst to better model the groundwater movement and solute transport in karst aquifers. Hence those processes are still poorly understood and understanding those processes requires innovative methods of investigation [17]. The heterogenous nature of karst aquifers which makes it hard to model and investigate also makes it hard to directly applied Darcy's equations for groundwater flow (used widely in hydrogeology and hydrogeological applications). Darcy's equations can work in an ideal karst aquifer which meets the requirements for Darcy's flow parameters, but not in most real aquifers [9, 17-19]. The residence time distribution function discussed in 1.1 is an innovative method that has been used to investigate karst aquifers. It is this method that will be discussed throughout this Thesis for analysis of a karst aquifer at Mammoth Cave National Park in Kentucky.

1.4 Thesis Problem Statement

The purpose of this project was to compare the gamma RTD model to the advection dispersion equation RTD model for a quantitative field tracer study performed at Mammoth Cave National Park, Kentucky.

1.5 Thesis Objective

The objective of this Thesis research was to determine whether the gamma RTD model is better than the advection dispersion equation RTD model at providing useful information derived from the RTD curve.

1.6 Thesis Techniques

First, the four parameter gamma RTD model was derived along with its first moment (mean residence time) and its second moment (variance or spread of the distribution). Second, a dye tracer study was performed at Mammoth Cave National Park to be able to produce a RTD curve. Third, the results of the tracer study were applied to the gamma, the advection dispersion equation, and the tracer RTD models. Using the mean-absolute deviation from the tracer RTD model, the best model would be determined, i.e., either the gamma or the advection dispersion equation RTD model.

1.7 Thesis Organization

Chapter 2 contains a discussion of the various theories involved in this Thesis research. Chapter 3 will discuss the dye tracer study completed at Mammoth Cave's *Shaler's Brook* and *Devil's Cooling Tub*. Chapter 4 will contain the data analysis of the tracer study. Chapter 5 contains the Conclusions and Recommendations for further research. Following Chapter 5 are the References. Appendix A, which follows the References, contains the raw quantitative tracer study data from *Shaler's Brook* and *Devil's Cooling Tub*. Appendix B includes the GNU Octave script and function M-files for computing the gamma RTD

function. Following the Appendices is the Biographical Sketch.

CHAPTER 2

NON-IDEAL FLOW LITERATURE REVIEW

2.1 Residence Time Distribution for Non-Ideal Flow Reactors

Researchers have used the distribution of residence times to examine the characteristics of a non-ideal flow reactor or system. The distribution of residence times or the residence time distribution (RTD) was first proposed to analyze chemical reactor performance in a paper by MacMullin and Weber in 1935 [1, 2, 3]. It was not until after Danckwerts' publication of "Continuous Flow Systems. Distribution of Residence Times," in 1953, that the RTD's theory was organized in a more structured manner and most of the distributions were classified [2-5]. Many people still use Danckwerts' work as their foundation for analysis of systems with the RTD model. The residence time distribution of a system characterizes the mixing that happens in a system and the quantity *E(t)* is the residence time distribution function. This function describes quantitatively the amount of time that different fluid particles have spent in the system. *E(t)* is also a probability density function (PDF) that defines the probability that a particle entering the system will remain there for a time *t* (see [1-8] for a thorough explanation of the background theory to mixing and RTD). Equation (1) is generally used to determine the RTD function [2, 7]

$$E(t)=\frac{C(t)}{\int_0^\infty C(t)\,dt}$$ (1), where C(t) is the concentration of the tracer over time and the plot

of C(t) versus time is the tracer breakthrough curve

It is important to note that all molecules will eventually leave the system (this is also a method used to normalize the distribution) [2, 3, 8], thus

$$\int_0^\infty E(t)\,dt = 1 \quad (2)$$

Two important parameters derived from the RTD function are the mean residence time (t_m) [2, 7]

$$t_m = \frac{\int_0^\infty tE(t)\,dt}{\int_0^\infty E(t)\,dt} = \int_0^\infty tE(t)\,dt \quad (3)$$

and the first moment about the mean of the RTD function (distribution variance or σ^2) [2]

$$\sigma^2 = \int_0^\infty (t - t_m)^2 E(t)\,dt \quad (4)$$

Although the RTD was originally applied to designing chemical reactors, the RTD has been used in a variety of other applications (see [1-9, 20-38] and their references for both a thorough discussion of the RTD and its widespread applications). The RTD has also been discussed in the literature as the detention time distribution (DTD) [39], transit time

distribution (TTD) [40], travel time distribution [41-43], and hydraulic residence time distribution (HRTD) [44-45]. Some researchers concentrate their efforts on obtaining the parameters derived from the RTD function to characterize the flow patterns that they are analyzing [46-47].

Generally, the main model used to describe the residence time distribution of a system has been the single parameter advection dispersion equation or model (ADE) [7, 9, 30, 32-38, 41, 43]. In the literature, the ADE has also been called the axial dispersion or diffusion equation or model (AxDE) or (ADM) [2, 3, 5-6, 8, 20-21, 24-26, 29]; the advection diffusion equation or "diffusion with bulk flow equation" [21]; or the convection dispersion or diffusion equation (CDE) [29, 48-49]. This model equation exhibits a RTD function curve which can appear Gaussian based on the conditions [30]. This model with its single parameter and Gaussian-shaped curves are inadequate for visualizing the non-ideal flow RTD [20, 30, 37-38]. Also, it is true that the symmetric ADE Gaussian-shaped curve predicts a finite tracer concentration at time = 0, but this is not true for the ADE solution at that time (see Chapters 4 and 5 for more details). Lastly, the ADE Gaussian-shaped curve does not fully display the fullness of tracer breakthrough curves that generally have long upper tails [37]. Thus, we decided to derive a RTD function for non-ideal flow systems by combining 2 two parameter gamma distributions. The gamma distribution resembles many natural processes and it has been used widely in complex applications thus it is a good model for non-ideal flow systems (see [39-43,

50-61] for both a thorough discussion of the gamma distribution and its various applications).

This jointly combined four parameter gamma model allows for more flexibility to account for the nonlinear aspects [40-41] of a non-ideal flow system than the single parameter ADE model; however, the gamma distribution's two parameters (α, β) do not have a clear physical interpretation associated with them [40] like the ADE model does with the Péclet number. To address this issue, the gamma distribution for the RTD was derived based on the assumption that the tracer travel distance and linear velocity of the system were gamma distributed random variables. This assumption solves the problems regarding the physical interpretation as $\alpha_1\beta_1$ is associated with the mean travel distance of the tracer molecules while $(\alpha_2\text{-}1)\beta_2$ is associated with the mean travel linear velocity (mean travel distance/mean time in the system). Thus we assume that the solute moves with the water. We also assume that the ratio $\alpha_1\beta_1/(\alpha_2\text{-}1)\beta_2$ is approximately equal to the mean residence time or the mean time in the system (t_m). The resulting four parameter model is robust and better able to fit the normalized tracer RTD curve (see Chapter 4 for the comparison of the normalized RTD curves). In addition, the model parameters' relationship to the linear velocity and the travel distance of the actual system simplifies the parametization of the model by reducing the degrees of freedom from four to two.

Regarding non-ideal flow systems, we are assuming the system is isothermal and homogeneous and that the volume changes during the tracer study are assumed to be

negligible [5-6]. We are also assuming that the time domain is steady state rather than transient. [2, 5-8] provides a thorough explanation of non-ideal flow systems. As discussed in Chapter 1, a karst aquifer is an example of non-ideal flow.

2.2 Derivation of the four parameter gamma RTD model

We are assuming that the residence time of tracer particles is similar to travel times of discrete water molecules in a non-ideal flow system along flow paths. The flow paths for discrete water particles vary in length and local hydraulic gradient and cross-section. Tracer sample concentration as a measure of the tracer flux at a given time is randomly distributed, but this paper does not apply a residence time distribution directly to the concentration data. Instead the arrival of molecules at the sampling point at a particular time is seen as a random event dependent on the distance it traveled and the speed at which it traveled. Thus, the relationship between travel distance and velocity reflected in the space time (τ) for a non-ideal flow system

$\tau = \frac{V_{eq}}{Q} = \frac{\bar{L} A_{eq}}{\bar{v} A_{eq}} = \frac{\bar{L}}{\bar{v}}$ (5), where both L and v represent independent random variables

For modeling non-ideal flow systems it is important to address the interaction of L and v because their independent values relate directly to important characteristics of the system. Specifically, distance traveled and the straight line distance between the injection and sampling point(s), localized hydraulic gradient(s), and flow cross-section(s) along the flow

path. It is for this reason that describing the tracer breakthrough curve in terms of a distribution derived from the joint PDF for L and v should provide better insight regarding the RTD for a non-ideal flow system.

The literature suggests that the gamma distribution does well in describing tracer breakthrough curves for non-ideal flow systems [37-39, 40-43]. The gamma distribution which is frequently used as a probability model for waiting times seems to adequately reflect the "long tail to the right" often observed in tracer breakthrough curves [33]. Based on this observation we assumed that L and v are independent random variables (irv) that have gamma PDFs as follows:

$$f_L(x_1)=\frac{x_1^{\alpha_1-1}e^{\frac{-x_1}{\beta_1}}}{\Gamma(\alpha_1)\beta_1^{\alpha_1}};\alpha_1\geq 1;\beta_1\geq 0,x_1\geq 0 \quad (6)$$

, where α_1 and β_1 are the shape and scale parameters of the two parameter gamma distribution, respectively and Γ(α) is the gamma function [50-55]

$$\Gamma(\alpha)=\int_0^{\infty} x^{\alpha-1}e^{-x}dx \quad (7)$$

$$f_v(x_2)=\frac{x_2^{\alpha_2-1}e^{\frac{-x_2}{\beta_2}}}{\Gamma(\alpha_2)\beta_2^{\alpha_2}};\alpha_2\geq 1;\beta_2\geq 0,x_2\geq 0 \quad (8)$$

, where α_2 and β_2 are the shape and scale parameters of the two parameter gamma distribution, respectively and Γ(α) is the gamma function [50-55]

$f(x)=\frac{x^{\theta-1}e^{\frac{-x}{\varphi}}}{\varphi^{\theta}\Gamma(\theta)};x>0;\theta,\varphi>0$ (9), this is the general formula for a two parameter gamma distribution where θ and φ are the shape and scale parameters of the distribution, respectively and Γ(θ) is the gamma function [62]

(The following mathematical discussion and Equations (10) – (16) are from [62]) "The distribution of residence time (t) is derived from the Mellin convolution of the distribution of quotients of random variables

where the PDF of the quotient

$Y=\frac{X_1}{X_2}=(X_1)\left(\frac{1}{X_2}\right)$ (10), where Y = t and X_1 = L and X_2 = v

of two nonnegative irv's with PDFs $f_L(x_1)$ and $f_v(x_2)$ is expressible as the Mellin convolution

$h_2(y)=\int_0^{\infty} x_2 f_L(yx_2) f_v(x_2)\,dx_2$ (11)

of $f_L(x_1)$ and $g_2(1/x_2)$. This is established by utilizing a transformation

$Y=\frac{X_1}{X_2},\quad X_2=X_2$ (12)

the inverse of which is

$$X_1 = YX_2, \quad X_2 = X_2 \text{ (13)}$$

As the Jacobian of the transformation (13) is

$$J = \begin{vmatrix} \frac{\partial x_1}{\partial y} & \frac{\partial x_1}{\partial x_2} \\ \frac{\partial x_2}{\partial y} & \frac{\partial x_2}{\partial x_2} \end{vmatrix} = \begin{vmatrix} x_2 & y \\ 0 & 1 \end{vmatrix} = x_2 \text{ (14)}$$

the joint PDF $f(x_1, x_2) = f_L(x_1)f_v(x_2)$ is transformed into $g(y, x_2)$, where

where

$$g(y, x_2) = f_L(yx_2) f_v(x_2) |J| = x_2 f_L(yx_2) f_v(x_2) \text{ (15)}$$

On integrating Equation (15) with respect to x_2, one obtains the Mellin convolution {in our case the PDF for the residence time (t) is given by the marginal probability in Equation (16)}

$$h_2(y) = \int_0^\infty g(y, x_2)\, dx_2 = \int_0^\infty x_2 f_L(yx_2) f_v(x_2)\, dx_2 \text{ (16)}$$

Equation (16) represents the PDF of the quotient random variable $Y = X_1/X_2$"

$$f_L(yx_2) = \frac{x_2 y^{\alpha_1 - 1} e^{\frac{-x_2 y}{\beta_1}}}{\Gamma(\alpha_1)\beta_1^{\alpha_1}} \text{ (17)}$$

$$f_v(x_2)=\frac{x_2^{\alpha_2-1}e^{\frac{-x_2}{\beta_2}}}{\Gamma(\alpha_2)\beta_2^{\alpha_2}} \quad (18)$$

$$h_2(y)=\int_0^{\infty} x_2\left(\frac{x_2 y^{\alpha_1-1}e^{\frac{-x_2 y}{\beta_1}}}{\Gamma(\alpha_1)\beta_1^{\alpha_1}}\right)\left(\frac{x_2^{\alpha_2-1}e^{\frac{-x_2}{\beta_2}}}{\Gamma(\alpha_2)\beta_2^{\alpha_2}}\right)dx_2 \quad (19)$$

make constant $C=\frac{y^{\alpha_1-1}}{\Gamma(\alpha_1)\Gamma(\alpha_2)\beta_1^{\alpha_1}\beta_2^{\alpha_2}}$ (20)

$$h_2(y)=C\int_0^{\infty} x_2^{\alpha_1+\alpha_2-1}e^{-x_2\left(\frac{y}{\beta_1}+\frac{1}{\beta_2}\right)}dx_2 \quad (21)$$

The solution to Equation (21) provides the PDF of the residence time or the combined four parameter gamma RTD model noted as E(t) in Equation (22)

$$E(t)=\frac{\Gamma(\alpha_1+\alpha_2)}{\Gamma(\alpha_1)(\alpha_2)}\left(\frac{\beta_1}{\beta_2}\right)^{\alpha_2}\left(\frac{t^{\alpha_1-1}}{\left(t+\frac{\beta_1}{\beta_2}\right)^{\alpha_1+\alpha_2}}\right);\ \alpha_1,\alpha_2,\beta_1,\beta_2\geq 0 \quad (22)$$

taking the first moment of Equation (22) about the mean using Equation (3) gives

$$t_m=\left(\frac{\beta_1}{\beta_2}\right)\left(\frac{\alpha_1}{\alpha_2-1}\right) \quad (23)$$

where the mean travel distance is

$$L=\alpha_1\beta_1 \quad (24)$$

and the mean travel linear velocity is

$$v=(\alpha_2-1)\beta_2 \quad (25)$$

Taking the second moment of Equation (22) about the mean using Equation (4) gives

$$\sigma^2=\left(\frac{\beta_1}{\beta_2}\right)^2\left(\frac{\alpha_1}{\alpha_2-1}\right)\left(\frac{\alpha_1+1}{\alpha_2-2}-\frac{\alpha_1}{\alpha_2-1}\right) \quad (26)$$

The individual distributions of L and v provide insight into predicting the characteristics of the transformed distribution.

Assistance in deriving the intermediate steps between Equations (21) and (22), between Equations (22) and (23), and between Equations (22) and (26) came from [63-66].

2.3 Advection Dispersion Equation RTD Model

The one parameter advection dispersion equation RTD model is obtained from the dimensionless effluent tracer concentration in Equation (27) which is derived from the solution to Danckwerts' "Open-Open System Boundary Conditions" and then applying Equation (1) to Equation (27) to produce Equation (28) [2, 3]

$$\Psi(1,\theta)=\frac{C_T(L,t)}{C_{T_0}}=\frac{1}{2\sqrt{\frac{\pi\theta}{Pe}}}\exp\left[\frac{-(1-\theta)^2}{\frac{4\theta}{Pe}}\right] \quad (27),$$ Equation (27) is derived in [2, 3]

$$E(t)=\frac{\Psi(1,\theta)}{\int_0^{\infty}\psi\, d\theta}$$ (28), Equation (28) is modified from the E(t) presented in [2, 7]

The Péclet number (Pe) in Equation (27) is computed via Equation (29) after both the mean residence time and the distribution variance are calculated

$$\frac{\sigma^2}{t_m^2}=\frac{2}{Pe}+\frac{8}{Pe^2}$$ (29), Equation (29) is derived in [2]

$$t_m=\left(1+\frac{2}{Pe}\right)\tau$$ (30), solving Equation (30) provides the space time (τ) [2]

CHAPTER 3

METHODS AND MATERIALS

3.1 Application of the Gamma RTD Function to a Karst Field Site

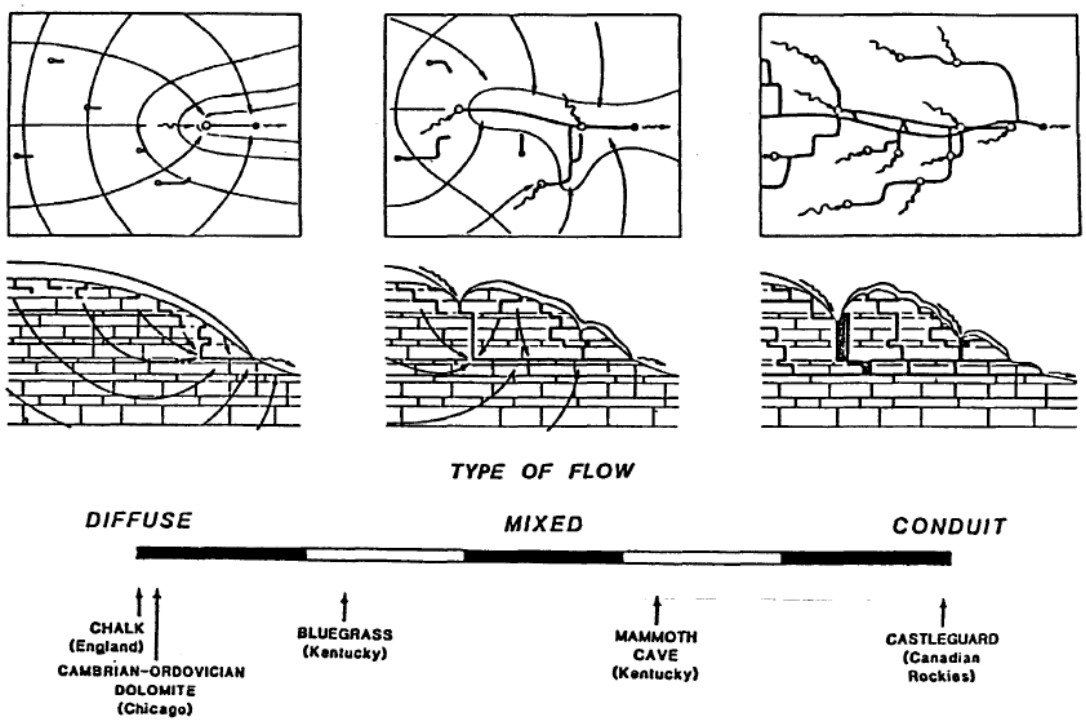

Figure 3.1 Diagram displays the types of flow possible in karst aquifers, from diffuse flow through mixed, to conduit flow [14]. This research was done at Mammoth Cave, Kentucky, which is considered a mix of diffuse and conduit flow, perhaps more conduit than diffuse. (adapted from [67])

The gamma RTD function was tested on the mixed flow karst aquifer at Mammoth Cave National Park, Kentucky (Figure 3.1).[1] Previous tracer studies performed at Mammoth

1The description of the diagram in Figure 3.1 follows: "The open circles indicate sinkholes that are water

Cave have contributed to our understanding of complex karst aquifers [14, 16, 68-69]. This quantitative tracer study furthers the goal to help us better understand the karst system with a new analytical RTD method based on the gamma distribution.

To determine the residence time distribution function a quantitative tracer study was performed with the fluorescent dye Rhodamine WT-20. The reader is referred to several review articles [14, 16, 46, 69-71] for a discussion of this and other tracer dyes. A method described by Mull et al., was modified to calculate the amount of rhodamine dye needed for this tracer study [14]. Equation (31) provides an estimate of the dye required to achieve a quantified dye study. Table 3.1 includes information that we used for D in Equation (31).

$$W_d = 1.478\sqrt{\left(\frac{DQ}{V}\right)} \quad (31)$$

where
W_d = the mass of the fluorescent dye in kg to be injected (Rhodamine WT-20)

D = straight-line distance in km from the injection point to the recovery point (Obtained from Table 3.1)

Q = discharge at the resurgence in m^3/s (Determined from discharge measurements in the cave)

V = estimated velocity of groundwater flow in m/hr

---

inputs. Blackened circles are springs. Wavy lines are surface streams. Heavy black lines are cave passages. Flow lines and equipotential lines are shown for diffuse flow and mixed flow, but the concept of such lines is not applicable in a purely conduit system." [14]

Table 3.1 Elevation and Distance Estimates for the Site Area

Description	**US Units**	**SI Units**
Dye input site elevation	751 ft	229 m
Shaler's Brook elevation	~538 ft	~164 m
Devil's Cooling Tub elevation	~558 ft	~170 m
Dye site to Shaler's Brook straightline horizontal distance	541 ft	165 m
Dye site to Shaler's Brook horizontal distance along surface stream	640 ft	~195 m
Dye site to Devil's Cooling Tub straightline horizontal distance	968 ft	~295 m
Note: all elevations are amsl – above mean sea level (2011)		

A Rhodamine WT-20 quantitative dye study was conducted to determine the travel time from the outlet of the Post Office filter to two receiving areas in the cave system, *Shaler's Brook* and *Devil's Cooling Tub*, which are indicated in Figure 3.2. The elevations and horizontal distances pertinent to better understanding Figure 3.2 and the dye study are included in Table 3.1.

On the afternoon of December 20, 2011, the dye study was prepared because it was scheduled to rain; however, the rain came much later (around 3 A.M. on December 21). A tipping delivery system was triggered by the rain event and released both salt and rhodamine dye. This set up is described more in Section 3.2.

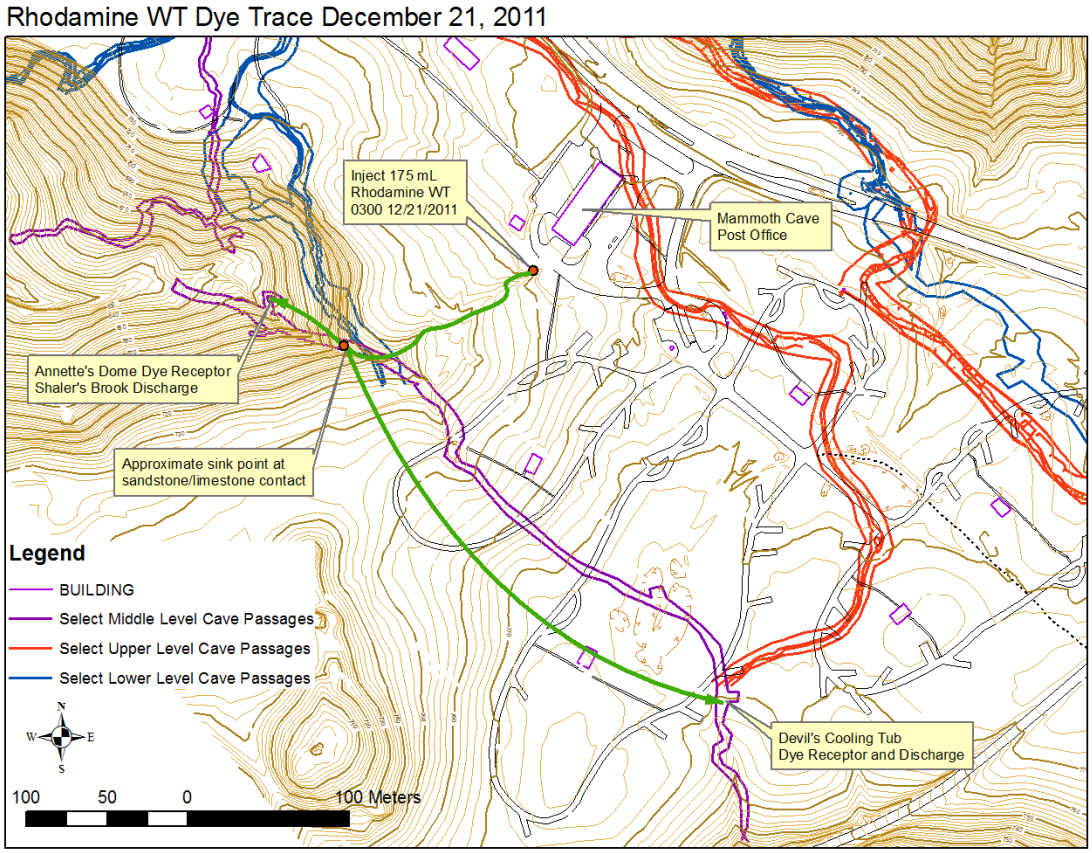

Figure 3.2 Topographic map of cave features with surface overlay. The green line represents the surface stream and a probable flow path of the dye to both Shaler's Brook and Devil's Cooling Tub. The red, blue, and purple lines delineate cave passages. (Courtesy of Dr. Rick Toomey at the Mammoth Cave International Center for Science and Learnina)

At the outlet of the stormwater treatment system, which services the Post Office parking lot, an ephemeral stream forms which drains into sinkholes downstream. The stream flow path and the approximate flow paths in the cave system are shown in Figure 3.2. Inside the cave, the stream has been shown to empty into an area known as *Annetta's Dome* (now

Annette's Dome) and portions are also entering into another area called *Devil's Cooling Tub*, both located approximately 200 feet beneath the surface. *Devil's Cooling Tub* and *Annette's Dome* were part of the cave tours during the early 1900's and tourists routinely drank from these flowing waters as part of their tour. Figure 3.3 provides approximate locations for *Devil's Cooling Tub*, *Annette's Dome*, and other important features in the cave system.

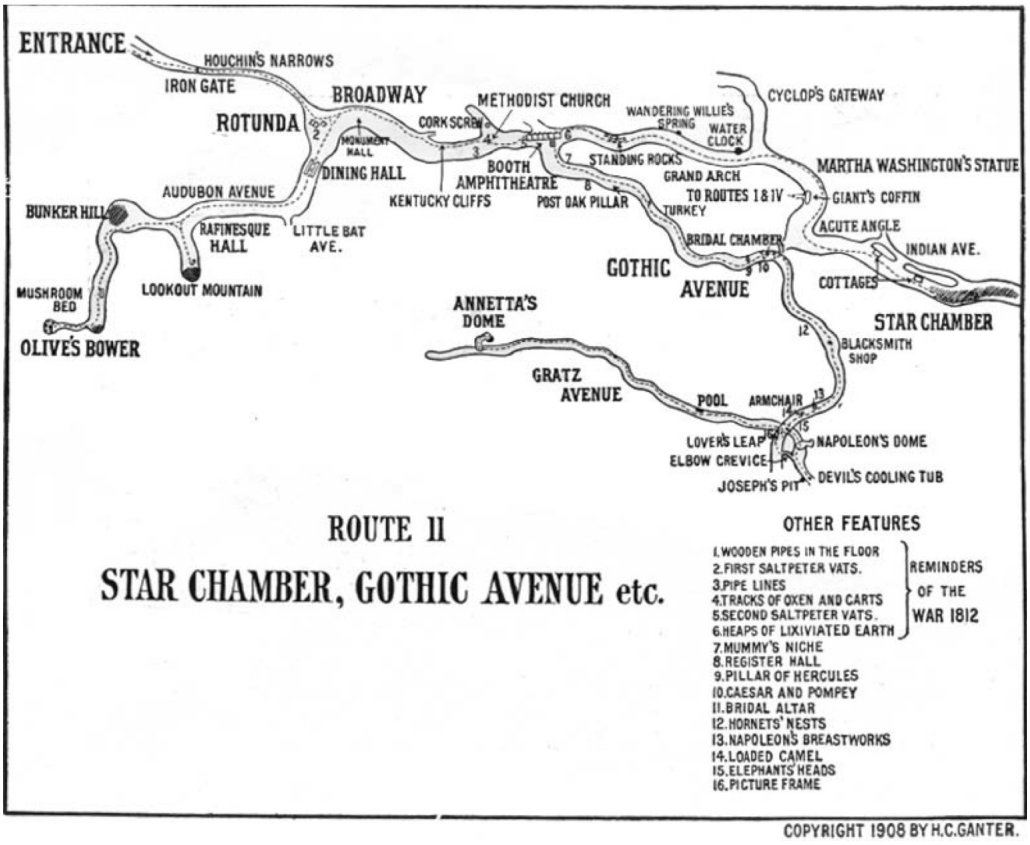

Figure 3.3 1908 Tour Map showing the 200 ft level of the cave showing cave features by their colloquial names, which are used to this day [72]. Annette's Dome (Annetta's Dome on the map) and Devil's Cooling Tub were referred to in this study. {Courtesy of Dr. Rick Toomey at the Mammoth Cave International Center for Science and Learning}

Annette's Dome creates another feature known as *Shaler's Brook*, located approximately 60 feet beneath the ceiling. *Shaler's Brook* receives direct discharge from *Annette's Dome*, therefore it is used as an endpoint in the dye study along with *Devil's Cooling Tub*. These subsurface areas were selected because previous tracer studies indicated relatively rapid rates of surface recharge at *Devil's Cooling Tub* and *Shaler's Brook*. At *Devil's Cooling*

Tub discharge rates ranged from 0.5 L/min to 51.95 L/min. On December 20, the average discharge measured was approximately 7 L/min. Discharge measurements for *Shaler's Brook* were taken at the formation known as *Lee's Cistern*, which receives direct discharge from *Shaler's Brook* approximately 50 yards downstream. *Lee's Cistern* discharge measurements ranged from 6.57 L/min to 176 L/min. On December 20, the average discharge in the *Annette's Dome-Shaler's Brook-Lee's Cistern* system measured was approximately 31 L/min.

3.2 Karst Dye Study Techniques

Discharge measurements were collected at *Lee's Cistern* and *Devil's Cooling Tub* at various dates preceding the quantitative dye tracer study. These discharge measurements were used to determine the amount of dye needed to avoid poor results from excessive dilution, but also remain within a safe range to preserve the karst ecosystem. We used a modified version of Equation (31) to calculate the mass of Rhodamine WT-20 fluorescent dye needed for this tracer study. At *Lee's Cistern*, discharge was measured using a plastic tarp to concentrate the stream and then recording the amount of time needed to fill a container of known volume. This was done in triplicate. At *Devil's Cooling Tub*, a similar procedure was followed to measure discharge.

The quantitative dye study was conducted on December 20, 2011, beginning on the surface at the outlet of a stormwater filter, which services parking lots adjacent to the Post Office on the park grounds. Inside the cave, fluorometers with rhodamine sensors and first

flush samplers were placed in two areas of the cave where they measured the amount of time taken by the dye to move through the karst system. The locations within the cave, *Shaler's Brook* and *Devil's Cooling Tub*, were selected because they were suspected to interact with the surface relatively rapidly and provide surface recharge for two major karst springs in the formation, Echo River and River Styx (see [68] for further discussion of the Mammoth Cave karst aquifer drainage basin divides). In addition to the Rhodamine WT-20 dye study, a salt tracer study was also conducted to gain additional hydrologic data. The tracers were placed on a release mechanism, see Figure 3.4 for the setup. The release mechanism consisted of a Styrofoam tray with approximately ¼ lb of table salt (114 g NaCl) laying flat on the tray & 175 mL of Rhodamine WT-20 in a plastic bottle standing upright on the tray. This mechanism was placed in the outlet of the storm filter system. Below, we placed a 1st flush sampler (white plastic container with the red lid) and a YSI datasonde (to measure the salt concentration) set to read every 5 minutes.

Figure 3.4 Photograph showing the dye and salt release mechanism. Also shown in the picture are the 1st flush sampler and the YSI datasonde.

Additional 1st flush samplers and datasondes with rhodamine sensors set to read at 20 minute intervals were placed in the cave. See Figure 3.5 to see the location of the YSI datasonde and the 1st flush sampler in *Shaler's Brook*. See Figure 3.6 to see the location of the GGUN-FL Fluorometer 80526 next to the YSI datasonde in *Devil's Cooling Tub*.

As the storm waters exited the filter, they reached a high enough velocity to flush the tray out & spill it. The tray was elevated approximately 0.5 inches in the discharge pipe to keep it from dumping on the very first trickle; rather, it needed enough flow to lift it & destabilize it. Based on the readings measured by the instruments, we concluded that the tracers were

released at approximately 3:00 A.M. on December 21, 2011 due to the rain event.

Figure 3.5 Photograph showing the pool at the bottom of Annette's Dome and the beginning of Shaler's Brook. Also pictured is the YSI datasonde (gray and yellow tube in water) and the 1st flush sampler (white gallon jar).

Figure 3.6 Picture showing the GGUN-FL Fluorometer 80526 next to the YSI datasonde in Devil's Cooling Tub on December 20, 2011.

CHAPTER 4

RESULTS

The results of the tracer study were used to develop the residence time distribution (RTD) function. The RTD function [E(t)] for contaminant molecules in a non-ideal flow system is a probability density function (PDF) which can be interpreted to define the probability that contaminant particles present in the influent at time equals zero will arrive at the effluent after a time. The RTD curve is depicted as a plot of E(t) versus time as time goes from zero to infinity (or a reasonably long time where the RTD approaches zero) [2-4, 6, 7, 8]. E(t) was determined by "injecting" a pulse of a conservative tracer (Rhodamine WT-20) into the stream leading into the karst aquifer via the release mechanism described in Chapter 3 at time (t) = 0 and then measuring the tracer concentration in the effluent as a function of time.

The raw data results of the quantitative dye study performed at Mammoth Cave National Park, specifically *Shaler's* Brook and *Devil's Cooling Tub* are included in Appendix A in Tables A.1 - A.3. Table A.1 includes the first 500 minutes of the tracer (dye) collection at *Shaler's Brook*. Tables A.2 and A.3 both include 8 hours of tracer collection at *Devil's Cooling Tub*. Table A.2 is for the first peak and Table 2.3 is for the second peak.

The aforementioned raw data were compiled in the Calc spreadsheet program of LibreOffice [73] to continue the analysis. In Calc, Equations (1), (3) – (4), and (27) – (28) were calculated for both the tracer RTD and the normalized tracer RTD models. Using the

Solver for Nonlinear Programming LibreOffice Calc extension [74], I computed the Péclet number (Pe) from Equation (29) using the DEPS (Differential Evolution & Particle Swarm Optimization) algorithm [75].

Equation (32) represents the solution to the one parameter advection dispersion equation residence time distribution function at time θ = 0. In this case the solution is Infinity, although a finite tracer concentration should be expected for the initial time interval. Therefore, to compare the 3 RTD models, I disregard the RTD at time = 0.

$$\Psi(1,\theta=0)=\frac{C_T(L,t)}{C_{T_0}}=\frac{1}{2\sqrt{\frac{\pi\times 0}{Pe}}}\exp\left[\frac{-(1-0)^2}{\frac{4\times 0}{Pe}}\right]\approx\infty \quad (32)$$

, Equation (32) is derived in [2, 3] and it is the same as Equation (27), except that θ = 0

and

$$E(t)=\frac{\Psi(1,\theta=0)}{\int_0^\infty \psi\, d\theta}\approx\infty \quad (33)$$

, Equation (33) is modified from the E(t) presented in [2, 7] and it is the same as Equation (28), except that E(t) is shown to be approximately equal to ∞

The normalized forms of the RTD for the tracer, the ADE model, and the gamma model were computed in LibreOffice Calc using normalized time. To determine the better RTD model, either the ADE or the gamma, I had to determine the mean-absolute deviation (MAD) [76], Equation (34), from the tracer RTD model.

$MAD = n^{-1} \sum_{i=1}^{n} |y_i - \hat{y}_i|$ (34), where n represents the number of values where y_i and $\hat{y}_i$ differ, y_i is either the value of the ADE or gamma RTD model, and $\hat{y}_i$ is the value of the tracer RTD model [76]

The MAD associated with the gamma RTD model was approximately 0.038 while the MAD for the ADE RTD model was approximately 0.16.

I computed the four parameters (α_1, β_1, α_2, β_2) to use in the gamma RTD model which provided a lower MAD than that produced from the ADE model using the DEPS algorithm. Both a script and function files [77] were written in the M-file language of the numerical computation program GNU Octave [78], which is an alternative to Mathworks' MATLAB®. Both the script and the function files are included in Appendix B. GNU Octave uses either the FLTK toolkit [79] or gnuplot [80] to produce its graphs. The following graphs in this article were created using gnuplot rather than the FLTK toolkit. The script and function files used the four parameters for the gamma RTD model to solve Equations (22) – (26) for the normalized gamma RTD model. The script and function files were also used to produce the graphs for the tracer breakthrough curve and the comparison of the normalized RTD curves. The results of the field quantitative tracer study using Rhodamine WT-20 are shown in the following figures: Figure 4.1 (*Shaler's Brook*), Figure 4.2 (*Devil's Cooling Tub* complete dye study), Figure 4.3 (*Devil's Cooling Tub* Peak 1), and Figure 4.4 (*Devil's Cooling Tub* Peak 2).

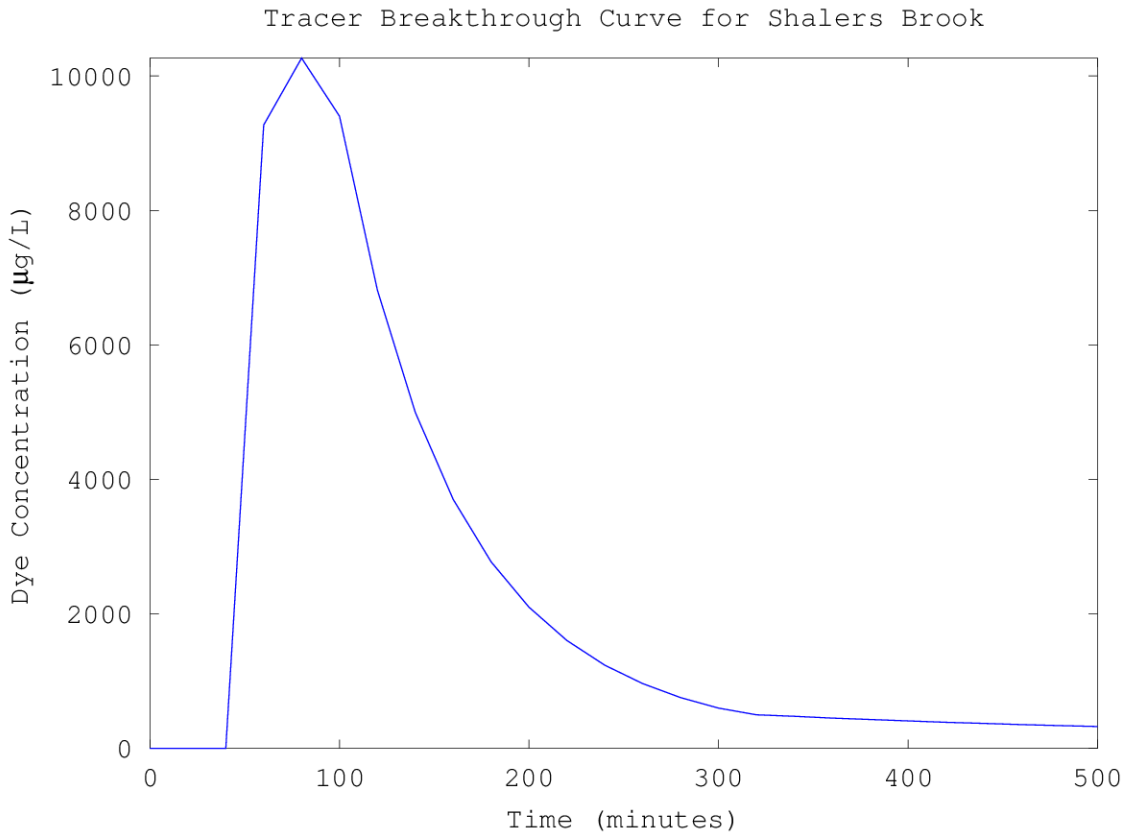

Figure 4.1 Tracer concentration versus time for the dye study at Shaler's Brook. This data was used to determine the mean. variance. and Péclet number for the karst system.

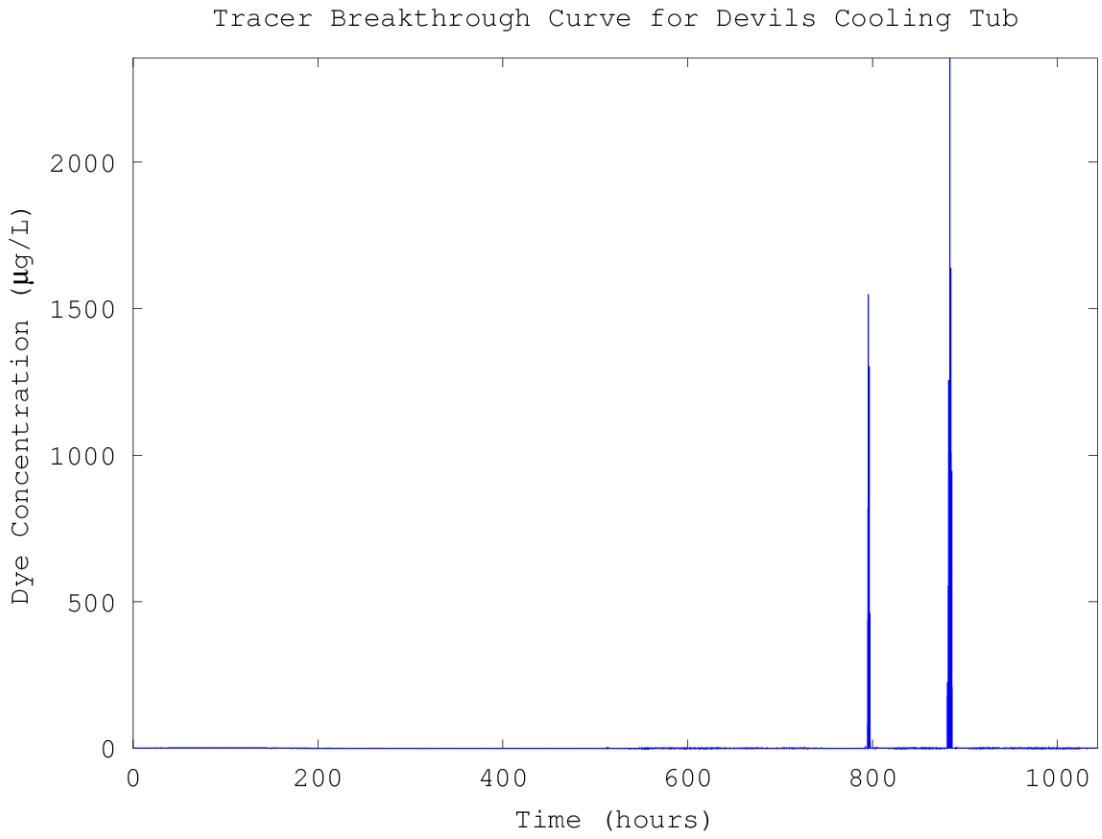

Figure 4.2 Tracer concentration versus time for the dye study at Devil's Cooling Tub.

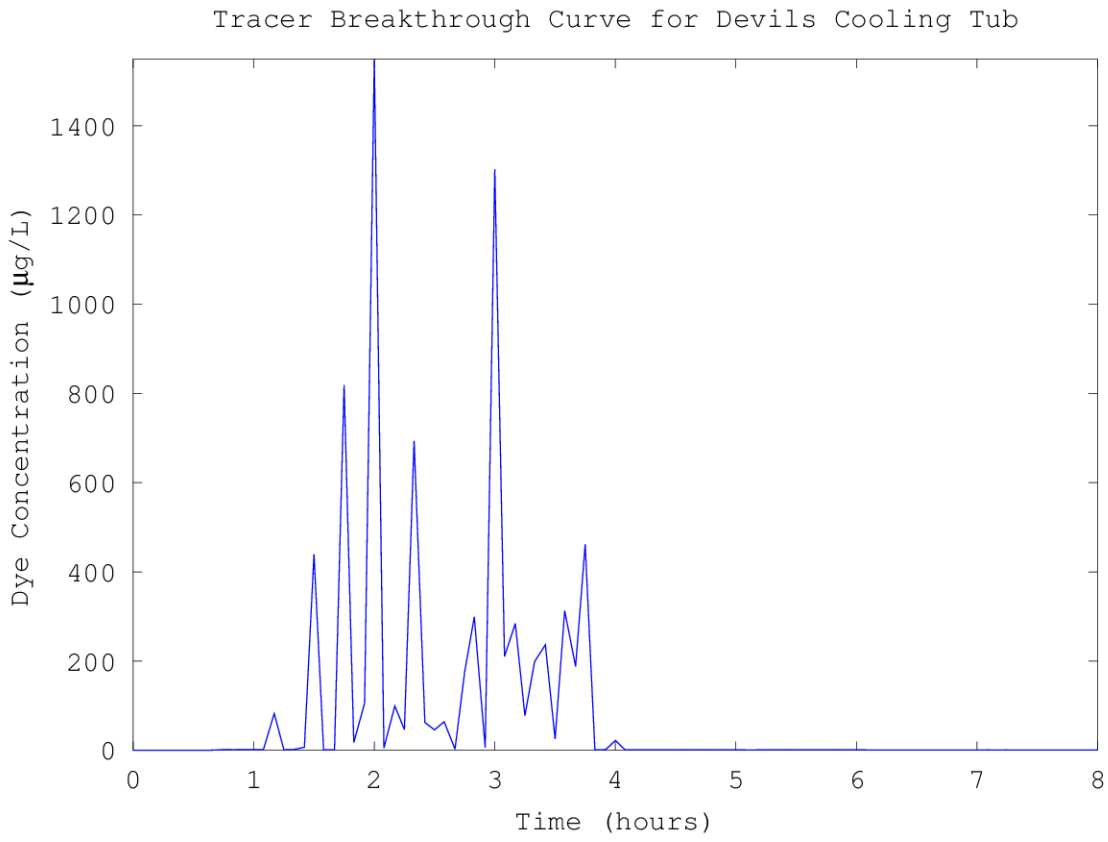

Figure 4.3 Tracer concentration versus time for the dye study at Devil's Cooling Tub. This figure provides a better view of the first peak.

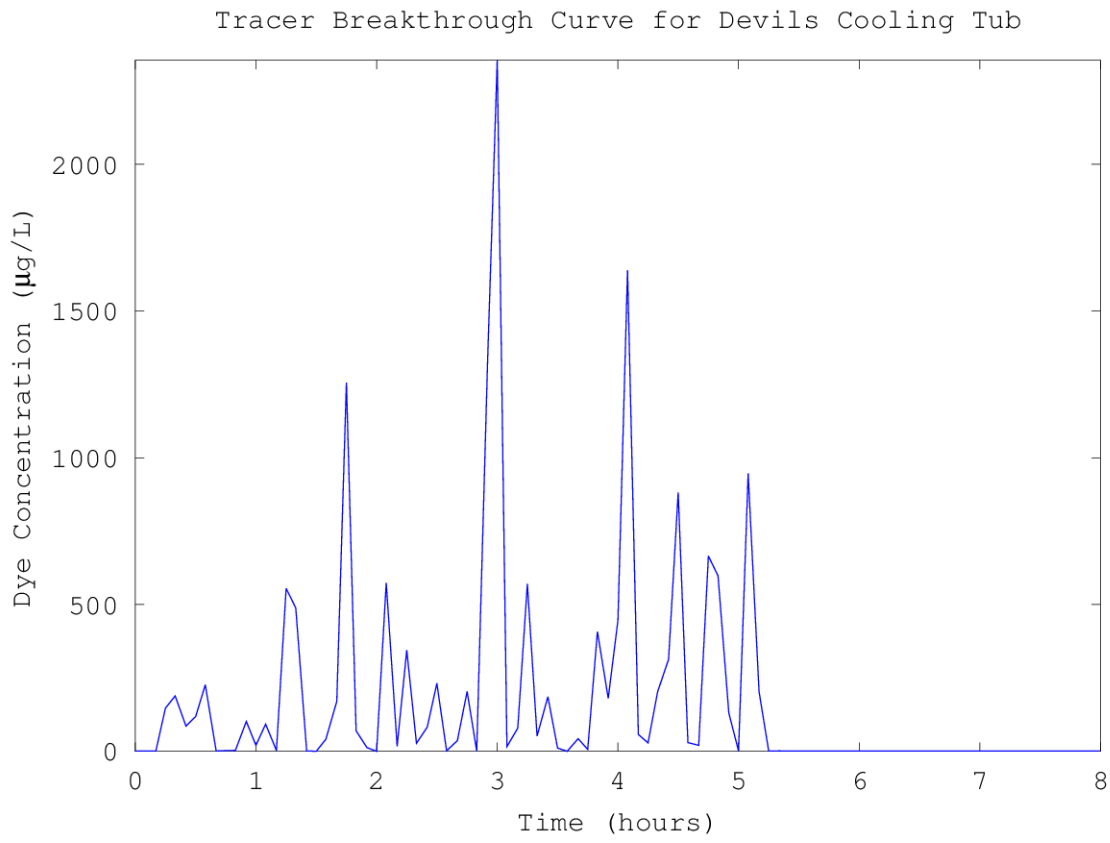

Figure 4.4 Tracer concentration versus time for the dye study at Devil's Cooling Tub. This figure provides a better view of the second peak.

The results for the field rhodamine dye study conducted at *Shaler's Brook* are: the mean residence time (t_m) is ≈ 140 minutes which is from Equation (3), the variance of the distribution (σ^2) is ≈ 7951 min^2 which is from Equation (4), the dimensionless Péclet number is ≈ 7.56 which is from Equation (29), and the space time (τ) is ≈ 111 minutes which is from Equation (30). The raw data for *Devil's Cooling Tub* was not analyzed in this study.

To compare the 2 RTD models to the tracer RTD from Equation (28) [gamma from Equation (22) and advection dispersion equation (ADE) from Equation (28)], I had to normalize each of the RTDs with dimensionless time.

Figure 4.5 shows the comparison of the normalized forms of the gamma RTD model and the ADE RTD model to the normalized tracer RTD model.

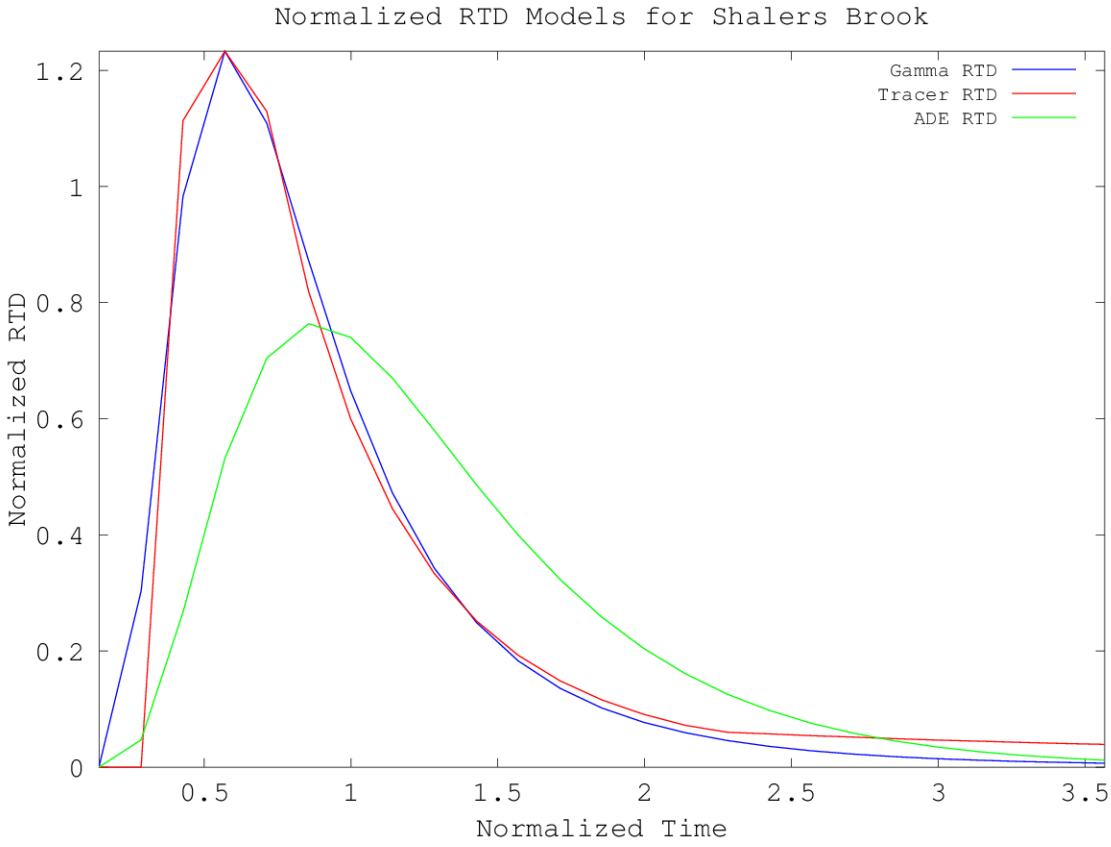

Figure 4.5 Comparing the normalized forms of the advection dispersion equation RTD and the gamma RTD models to the normalized tracer RTD model for the field tracer study at Shaler's Brook.

The results for the normalized gamma RTD model's interpretation of the field tracer study

conducted at *Shaler's Brook* using $\alpha_1 \approx 37$, $\alpha_2 \approx 4.6$, $\beta_1 \approx 4.5$, and $\beta_2 \approx 50$ are as follows: The dimensionless mean residence time or mean time in the system (t_m) is ≈ 0.92 mean minutes which is from Equation (23), the mean travel distance of tracer molecules is ≈ 165 mean meters which is from Equation (24), the mean travel linear velocity (mean travel distance of tracer molecules/mean time in the system) is ≈ 179 mean meters/minute which is from Equation (25), and the dimensionless variance of the distribution (σ^2) is ≈ 0.36 mean min^2 which is from Equation (26).

CHAPTER 5

CONCLUSION

The purpose of this project was to compare the gamma RTD model to the advection dispersion equation RTD model for a quantitative field tracer study performed at Mammoth Cave National Park, Kentucky. The objective of this Thesis research was to determine whether the gamma RTD model is better than the advection dispersion equation RTD model at providing useful information derived from the RTD curve.

The one parameter advection dispersion equation RTD model is obtained from the dimensionless effluent tracer concentration in Equation (27) which is derived from the solution to Danckwerts' "Open-Open System Boundary Conditions" and then applying Equation (1) to Equation (27) to produce Equation (28). Equation (27) includes the Péclet number which means that the ADE RTD model can be related back to a physical quantity. The four parameter gamma RTD model in Equation (22) was obtained from joining two-two parameter gamma distributions based on the tracer travel distance from Equation (6) and the tracer linear velocity from Equation (8). As the gamma RTD model is related back to time (length/velocity) via the physical site, the gamma RTD model is related back to a physical quantity. Both the advection dispersion equation RTD and the gamma RTD were used to analyze the non-ideal flow system in Mammoth Cave. Figure 4.5 shows both normalized forms of the gamma RTD and the ADE RTD compared to the normalized form of the tracer RTD. Both the tracer RTD and the gamma RTD curves display the long tail

to the right that is common in tracer curves, but the ADE RTD curve does not as it is Gaussian-shaped.

The gamma RTD function provides information that the ADE RTD function cannot. The normalized gamma RTD function allows for the calculation of the mean travel linear velocity and the mean travel distance which are obtained from the α and β parameters obtained from the best fit of the normalized gamma RTD to the normalized tracer RTD. The dimensionless mean residence time or mean time in the system (t_m) is ≈ 0.92 mean minutes which is from Equation (23), the mean travel distance of tracer molecules is ≈ 165 mean meters which is from Equation (24), the mean travel linear velocity (mean travel distance of tracer molecules/mean time in the system) is ≈ 179 mean meters/minute which is from Equation (25), and the dimensionless variance of the distribution (σ^2) is ≈ 0.36 mean min^2 which is from Equation (26). A mean residence time of ≈ 0.92 mean minutes means that the probability density function or the residence time distribution function for this field site is not a true PDF as the area under of the curve should be equal to 1 mean minute (or other mean time units), refer back to Equation (2). The mean travel distance of ≈ 165 mean meters is equal to the straightline horizontal distance from the inlet to the outlet at *Shaler's Brook*.

As previously discussed in Chapter 4, the initial time value had to be removed from the comparison of the three normalized RTD models due to the normalized ADE RTD function computing a value of ∞ at this time. This flaw presents a major setback in using

the one parameter advection dispersion equation RTD function.

The normalized forms of the gamma RTD and the advection dispersion equation RTD were compared with the normalized tracer RTD. The normalized gamma RTD function had a lower mean-absolute deviation (MAD) than the normalized advection dispersion equation when compared to the normalized tracer RTD function. As aforementioned in Chapter 4, the mean-absolute deviation (MAD) from the normalized tracer RTD function for the normalized gamma RTD function was ≈ 0.038 compared to ≈ 0.16 for the normalized ADE RTD model. The lower MAD value for the normalized gamma RTD function was also displayed visually in Figure 4.5. The gamma RTD function is tied back to the actual physical site due to its randomly distributed variables. This verification suggests that the gamma RTD function is a suitable alternative to the advection dispersion equation RTD function for quantitative tracer studies of karst aquifers and other non-ideal flow systems.

RECOMMENDATIONS FOR FURTHER RESEARCH

I recommend that the following future research be conducted:

- Analyze the *Devil's Cooling Tub* dye study data with the gamma RTD model
- Derive the relationship between the gamma RTD model and a first order biodegradation rate (mean conversion) using numerical integration
- Analyze the individual length and velocity gamma distributions and their relationship to the tracer RTD

- Use the gamma RTD to analyze other non-ideal flow systems, such as bioretention facilities (rain gardens), rivers, air systems, etc.
- Develop a software application that will use the gamma RTD model as its foundation to aid in the analysis of quantitative tracer studies. This program would be similar to QTRACER2, but it would be based off of the gamma RTD rather than the ADE RTD. I suggest developing this application in conjunction with other College of Engineering Departments and other Universities (Syracuse University, Tennessee Technological University, University of Arkansas, Vanderbilt University, Middle Tennessee State University, and/or University of Tennessee, etc.)

REFERENCES

1. R. B. MacMullin and M. Weber, “The theory of short-circuiting in continuous-flow mixing vessels in series and kinetics of chemical reactions in such systems,” *Transactions of American Institute of Chemical Engineers*, vol. 31, no. 2, pp. 409-458, 1935.

2. H. S. Fogler, *Elements of Chemical Reaction Engineering*, Prentice Hall PRT, Upper Saddle River, New Jersey, USA, 3rd Edition, 1999.

3. O. Levenspiel, *Chemical Reaction Engineering*, 3rd Edition, John Wiley & Sons, Inc., New York, New York, USA, 1999.

4. P. V. Danckwerts, “Continuous flow systems. Distribution of residence times,” *Chemical Engineering Science*, vol. 2, no. 1, pp. 1-13, 1953. http://www.sciencedirect.com/science/article/pii/0009250953800011

5. R. Shinnar and P. Naor, “Residence time distributions in systems with internal reflux,” *Chemical Engineering Science*, vol. 22, no. 10, pp. 1369-1381, 1967. http://www.sciencedirect.com/science/article/pii/0009250967800277

6. C. G. Hill, Jr., *An Introduction to Chemical Engineering Kinetics & Reactor Design*, John Wiley & Sons, Inc., New York, New York, USA, 1977.

7. G. Tchobanoglous, F. L. Burton, H. D. Stensel, and Metcalf & Eddy, Inc., *Wastewater Engineering: Treatment and Reuse*, 4th Edition, The McGraw-Hill Companies, Inc., New York, New York, USA, 2003.

8. L. D. Schmidt, *The Engineering of Chemical Reactions*, Oxford University Press, New York, New York, USA, 1998.

9. R. Painter, T. Byl, L. Sharpe, V. Watson, and T. Patterson, “A residence time distribution approach to biodegradation in fuel impacted karst aquifers,” J*ournal of Civil & Environmental Engineering*, vol. 2, no. 5, 2012. http://www.omicsgroup.org/journals/ArchiveJCEE/articleinpressJCEE.php#?%20aid=7137

10. United States Geological Survey (USGS) Groundwater Information, “What is Karst?” [online] Available: http://water.usgs.gov/ogw/karst/pages/whatiskarst, (Date- April 12, 2011)

11. United States Department of the Interior National Atlas of the United States, "Engineering Aspects of Karst" [online] Available: http://nationalatlas.gov/mld/karst0m.html, (Date- April 12, 2011)

12. M. R. Ralston and I. S. Oweis, "Geotechnical Engineering Considerations for Stormwater Management in Karst Terrain," 1*999 Southeastern Pennsylvania Stormwater Management Symposium – Implementing Best Management Practices*, October 20-21, 1999, Villanova University.

13. J. All, R. Elrod, J. Goldsmith, and P. Kambesis, "Stormwater Remediation in a Karst Watershed: A case study from Bowling Green, KY," *Stormwater*, Journal for Surface Water Quality Professionals, May 2009. [online] Available: http://www.stormh2o.com/SW/Articles/Stormwater_Remediation_in_a_Karst_Watershed_6084.aspx (Date- March 16, 2011)

14. D. S. Mull, T. D. Liebermann, J. L. Smoot, L. H. Woosley, Jr., *Application of Dye-Tracing Techniques for Determining Solute-Transport Characteristics of Ground Water in Karst Terranes*, United States Environmental Protection Agency Region 4, EPA 904/6-88-001, 1988. http://oaspub.epa.gov/eims/eimscomm.getfile?p_download_id=36351

15. United States Geological Survey (USGS) Karst Applied Research Studies Through Geologic Mapping (KARST) Project, "Karst Project, National Karst Map Task" [online] Available: http://geology.er.usgs.gov/eespteam/Karst/tasks/karstmap/karstmap.html, (Date- April 12, 2011)

16. M. Ryan and J. Meiman, "An examination of short-term variations in water quality at a karst spring in Kentucky," *Ground Water,* vol. 34, no. 1, pp. 23-30, 1996. http://onlinelibrary.wiley.com/doi/10.1111/j.1745-6584.1996.tb01861.x/abstract

17. M. S. Field, "Risk assessment methodology for karst aquifers: (2) solute-transport modeling," *Environmental Monitoring and Assessment*, vol. 47, no. 1, pp. 23-37, 1997. http://www.springerlink.com/content/xw564h0v422p0070/?MUD=MP

18. D. Ford and P. Williams, *Karst Hydrogeology and Geomorphology*, Revised Edition, John Wiley & Sons, Hoboken, New Jersey, USA, 2007.

19. Edited by N. Goldscheider and D. Drew, *Methods in Karst Hydrogeology*, Taylor & Francis, New York, New York, USA, 2007.

20. V. K. Pareek, R. Sharma, C. Cooper, and A. Adesina, “Solids residence time distribution in a three-phase bubble column reactor: An artificial neural network analysis,” *The Open Chemical Engineering Journal*, vol. 2, pp. 73-78, 2008. http://www.benthamscience.com/open/tocengj/articles/V002/73TOCENGJ.htm

21. J. Čermáková, F. Scargiali, N. Siyakatshana, V. Kudrna, A. Brucato, and V. Machoň, “Axial dispersion model for solid flow in liquid suspension in system of two mixers in total recycle,” *Chemical Engineering Journal*, vol. 117, no. 2, pp. 101-107, 2006. http://www.sciencedirect.com/science/article/pii/S138589470500361X

22. C. Laquerbe, J. Laborde, S. Soares, L. Ricciardi, P. Floquet, L. Pibouleau, and S. Domenech, “Computer aided synthesis of RTD models to simulate the air flow distribution in ventilated rooms,” *Chemical Engineering Science*, vol. 56, no. 20, pp. 5727-5738, 2001. http://www.sciencedirect.com/science/article/pii/S0009250901002925

23. S. Javid Royaee and M. Sohrabi, “Comprehensive study on wastewater treatment using photo-impinging streams reactor: Residence time distribution and reactor modeling,” *Industrial & Engineering Chemistry Research*, vol. 51, no. 11, pp. 4152-4160, 2012. http://pubs.acs.org/doi/abs/10.1021/ie201384s

24. J. C. Williams and M. A. Rahman, “The continuous mixing of particulate solids,” *Journal of the Society of Cosmetic Chemists*, vol. 21, no. 1, pp. 3-36, 1970. http://journal.scconline.org/abstracts/cc1970/cc021n01/p00003-p00036.html

25. C. G. C. C. Gutierrez, E. F. T. S. Dias, and J. A. W. Gut, “Investigation of the residence time distribution in a plate heat exchanger with series and parallel arrangements using a non-ideal tracer detection technique,” *Applied Thermal Engineering*, vol. 31, no. 10, pp. 1725-1733, 2011. http://www.sciencedirect.com/science/article/pii/S1359431111000950

26. C. G. C. C. Gutierrez, E. F. T. S. Dias, and J. A. W. Gut, “Residence time distribution in holding tubes using generalized convection model and numerical convolution for non-ideal tracer detection,” *Journal of Food Engineering*, vol. 98, no. 2, pp. 248-256, 2010. http://www.sciencedirect.com/science/article/pii/S0260877410000063

27. A. P. Torres and F. A. R. Oliveira, “Residence time distribution studies in continuous thermal processing of liquid foods: a review,” *Journal of Food Engineering*, vol. 36, no. 1, pp. 1-30, 1998. http://www.sciencedirect.com/science/article/pii/S0260877498000375

28. M. E. Rodrigues, A. R. Costa, M. Henriques, J. Azeredo, and R. Oliveira, “Wave

characterization for mammalian cell culture: residence time distribution," *New Biotechnology*, vol. 29, no. 3, pp. 402-408, 2012. http://www.sciencedirect.com/science/article/pii/S1871678411002263

29. J. B. Bassingthwaighte, "Physiology and theory of tracer washout techniques for the estimation of myocardial blood flow: Flow estimation from tracer washout," *Progress in Cardiovascular Diseases*, vol. 20, no. 3, pp. 165-189, 1977. http://www.ncbi.nlm.nih.gov/pmc/articles/PMC3021479/

30. J. N. Carleton, *Modeling Approaches for Treatment Wetlands*. Dissertation. University of Maryland, College Park, 2009. http://hdl.handle.net/1903/9585

31. J. N. Carleton, and H. J. Montas, "A modeling approach for mixing and reaction in wetlands with continuously varying flow," *Ecological Engineering*, vol. 29, no. 1, pp. 33-44, 2007. http://www.sciencedirect.com/science/article/pii/S0925857406001510

32. J. N. Carleton, and H. J. Montas, "An analysis of performance models for free water surface wetlands," *Water Research*, vol. 44, no. 12, pp. 3595-3606, 2010. http://www.sciencedirect.com/science/article/pii/S0043135410002484

33. Z.-Q. Deng, H.-S. Jung, and B. Ghimire, "Effect of channel size on solute residence time distributions in rivers," *Advances in Water Resources*, vol. 33, no. 9, pp. 1118-1127, 2010. http://www.sciencedirect.com/science/article/pii/S0309170810001284

34. R. A. Payn, M. N. Gooseff, D. A. Benson, O. A. Cirpka, J. P. Zarnetske, W. B. Bowden, J. P. McNamara, and J. H. Bradford, "Comparison of instantaneous and constant-rate stream tracer experiments through non-parametric analysis of residence time distributions," *Water Resources Research*, vol. 44, no. 6, W06404, 10 pages, 2008. http://www.agu.org/pubs/crossref/2008/2007WR006274.shtml

35. R. Painter, T. Byl, L. Sharpe, A. Kheder, and J. Harris, "The role of attached and free-living bacteria in biodegradation in karst aquifers," *Water*, vol. 3, pp. 1139-1148, 2011. http://www.mdpi.com/2073-4441/3/4/1139

36. T. D. Byl and R. Painter, "Microbial adaptations to karst aquifers with contaminants," *Proceedings of the 19th Tennessee American Water Resources Association (AWRA) Tennessee Water Resources Symposium*, Burns, Tennessee, USA, pp. 2C-9--2C-12, 2009.

37. M. Martin and R. Painter, "Use of independent gamma distribution to describe tracer

break-through curves," *Proceedings of the 19th Tennessee American Water Resources Association (AWRA) Tennessee Water Resources Symposium*, Burns, Tennessee, USA, pp. P-10--P-10, 2009.

38. I. Embry, V. Roland, R. Painter, R. Toomey, and L. Sharpe, "Quantitative dye tracing – development of a new interpretative method," *Proceedings of the 22nd Tennessee American Water Resources Association (AWRA) Tennessee Water Resources Symposium*, Burns, Tennessee, USA, pp. 1C-6--1C-16, 2012.

39. R. H. Kadlec, "Effects of pollutant speciation in treatment wetlands design," *Ecological Engineering*, vol. 20, no. 1, pp. 1-16, 2003. http://www.sciencedirect.com/science/article/pii/S0925857402001180

40. M. Hrachowitz, C. Soulsby, D. Tetzlaff, I. A. Malcolm, and G. Schoups, "Gamma distribution models for transit time estimation in catchments: Physical interpretation of parameters and implications for time-variant transit time assessment," *Water Resources Research*, vol. 46, no. 10, W10536, 15 pages, 2010. http://www.agu.org/pubs/crossref/2010/2010WR009148.shtml

41. J. W. Kirchner, X. Feng, and C. Neal, "Catchment-scale advection and dispersion as a mechanism for fractal scaling in stream tracer concentrations," *Journal of Hydrology*, vol. 254, no. 1-4, pp. 82-101, 2001. http://www.sciencedirect.com/science/article/pii/S0022169401004875

42. J. W. Kirchner, D. Tetzlaff, and C. Soulsby, "Comparing chloride and water isotopes as hydrological tracers in two Scottish catchments," *Hydrological Processes*, vol. 24, no. 12, pp. 1631-1645, 2010. http://onlinelibrary.wiley.com/doi/10.1002/hyp.7676/abstract

43. J. W. Kirchner, X. Feng, and C. Neal, "Fractal stream chemistry and its implications for contaminant transport in catchments," *Nature*, vol. 403, no. 6769, pp. 524-527, 2000. http://www.nature.com/nature/journal/v403/n6769/full/403524a0.html

44. A. Brovelli, O. Carranza-Diaz, L. Rossi, and D. Barry, "Design methodology accounting for the effects of porous medium heterogeneity on hydraulic residence time and biodegradation in horizontal subsurface flow constructed wetlands," *Ecological Engineering*, vol. 37, no. 5, pp. 758-770, 2011. http://www.sciencedirect.com/science/article/pii/S0925857410001382

45. V. Zahraeifard and Z. Deng, "Hydraulic residence time computation for constructed wetland design," *Ecological Engineering*, vol. 37, no. 12, pp. 2087-2091, 2011.

http://www.sciencedirect.com/science/article/pii/S0925857411002746

46. M. S. Field, *The QTRACER2 Program for Tracer Break-through Curve Analysis For Tracer Tests in Karst Aquifers and Other Hydrologic Systems*, U. S. Environmental Protection Agency, Office of Research and Development, EPA/600/R-02/001, 2002. http://oaspub.epa.gov/eims/eimscomm.getfile?p_download_id=36351

47. M. S. Field, "Efficient hydrologic tracer-test design for tracer-mass estimation and sample-collection frequency, 1. method development," *Environmental Geology*, vol. 42, no. 7, pp. 827-838, 2002. http://dx.doi.org/10.1007/s00254-002-0591-2

48. B. Zhou, Y. Jiang, Q. Wang, and M. Shao, "Chloride transport in undisturbed soil columns of the Loess Plateau," *African Journal of Agricultural Research*, vol. 6, no. 20, pp. 4807-4815, 2011.
http://www.academicjournals.org/ajar/abstracts/abstracts/abstracts2011/26%20Sept/Zhou%20et%20al.htm

49. M. Vanclooster, D. Mallants, J. Diels, and J. Feyen, "Determining local-scale solute transport parameters using time domain reflectometry (TDR)," *Journal of Hydrology*, vol. 148, no. 1-4, pp. 93-107, 1993.
http://www.sciencedirect.com/science/article/pii/0022169493902547

50. R. D. Markovic, "Probability functions of best fit to distributions of annual precipitation and runoff," *Hydrology Papers* No. 8 (August 1965), Colorado State University, Fort Collins, Colorado, USA, 1965.

51. I. Kotlarski, "On characterizing the gamma and the normal distribution," *Pacific Journal of Mathematics*, vol. 20, no. 1, pp. 69-76, 1967.
http://projecteuclid.org/DPubS?service=UI&version=1.0&verb=Display&handle=euclid.pjm/1102992970

52. A. Stuart and K. Ord, *Kendall's Advanced Theory of Statistics: Volume 1: Distribution Theory*, 6th Edition, Oxford University Press Inc., New York, New York, USA, 1994.
53. K. V. Bury, *Statistical Distributions in Engineering*, Cambridge University Press, New York, New York, USA, 1999.

54. N. T. Kottegoda and R. Rosso, *Statistics, Probability, and Reliability for Civil and Environmental Engineers*, The McGraw-Hill Companies, Inc., New York, New York, USA, 1997.

55. B. Bobée and F. Ashkar, *The Gamma Family and Derived Distributions Applied in Hydrology*, Water Resources Publications, Littleton, Colorado, 1991.

56. H. A. Loáiciga, "Residence time, groundwater age, and solute output in steady-state groundwater systems," *Advances in Water Resources*, vol. 27, no. 7, pp. 681-688, 2004. http://www.sciencedirect.com/science/article/pii/S030917080400082X

57. S. K. Singh, "Simplified use of gamma-distribution/Nash model for runoff modeling," *Journal of Hydrologic Engineering*, vol. 9, no. 3, pp. 240-243, 2004. http://ascelibrary.org/doi/abs/10.1061/%28ASCE%291084-0699%282004%299%3A3%28240%29

58. S. Yue, "A bivariate gamma distribution for use in multivariate flood frequency analysis," *Hydrological Processes*, vol. 15, no. 6, pp. 1033-1045, 2001. http://onlinelibrary.wiley.com/doi/10.1002/hyp.259/abstract

59. H. Aksoy, "Use of gamma distribution in hydrological analysis," *Turkish Journal of Engineering and Environmental Sciences*, vol. 24, no. 6, pp. 419-428, 2000. http://mistug.tubitak.gov.tr/bdyim/abs2.php?dergi=muh&rak=9909-13

60. I. E. Amin and M. E. Campana, "A general lumped parameter model for the interpretation of tracer data and transit time calculation in hydrologic systems," *Journal of Hydrology*, vol. 179, no. 1-4, pp. 1-21, 1996. http://www.sciencedirect.com/science/article/pii/0022169495028803

61. P. Bhunya, R. Berndtsson, C. Ojha, and S. Mishra, "Suitability of gamma, chi-square, weibull, and beta distributions as synthetic unit hydrographs," *Journal of Hydrology*, vol. 334, no. 1-2, pp. 28-38, 2007. http://www.sciencedirect.com/science/article/pii/S0022169406005075

62. M. D. Springer, *The Algebra of Random Variables*, John Wiley & Sons, Inc., New York, New York, USA, 1979.

63. G. A. Korn and T. M. Korn, *Mathematical Handbook for Scientists and Engineers: Definitions, Theorems, and Formulas for Reference and Review*, 2nd enlarged and revised Edition, McGraw-Hill Book Company, New York, New York, USA, 1968.

64. S. M. Selby, *CRC Standard Mathematical Tables*, 18th Edition, The Chemical Rubber Co., Cleveland, Ohio, USA, 1970.

65. A. Jeffrey, *Handbook of Mathematical Formulas and Integrals*, 3rd Edition, Elsevier Academic Press, New York, New York, USA, 2004.

66. Edited by D. Zwillinger, S. G. Krantz, and K. H. Rosen, *CRC Standard Mathematical Tables and Formulae*, 30th Edition, CRC Press, Inc., New York, New York, USA, 1995.

67. J. F. Quinlan and R. O. Ewers, "Ground water flow in limestone terranes: Strategy rationale and procedure for reliable, efficient monitoring of ground water quality in karst area," *Proceedings of the Fifth National Symposium and Exposition on Aquifer Restoration and Ground Water Monitoring*, National Water Well Association, Worthington, Ohio, USA, pp, 197-234.

68. J. Meiman, C. Groves, and S. Herstein, "In-Cave Dye Tracing and Drainage Basin Divides in the Mammoth Cave Karst Aquifer, Kentucky," *U. S. Geological Survey Karst Interest Group Proceedings*, pp. 179-185, 2001.
http://water.usgs.gov/ogw/karst/kigconference/jm_incavedye.htm

69. N. Goldscheider, J. Meiman, M. Pronk, C. Smart, "Tracer tests in karst hydrogeology and speleology," *International Journal of Speleology*, vol. 37, no. 1, pp. 27-40, 2008.
http://www.ijs.speleo.it/article.php?id_art=556

70. H. Behrens, U. Beims, H. Dieter, G. Dietze, T. Eikmann, T. Grummt, H. Hanisch, H. Henseling, W. Käß, H. Kerndorff, C. Leibundgut, U. Müller-Wegener, I. Rönnefahrt, B. Scharenberg, R. Schleyer, W. Schloz, and F. Tilkes, "Toxicological and ecotoxicological assessment of water tracers," *Hydrogeology Journal*, vol. 9, no. 3, pp. 321-325, 2001.
http://dx.doi.org/10.1007/s100400100126

71. Field, Malcolm S., "Assessing Aquatic Ecotoxicological Risks Associated with Fluorescent Dyes Used for Water-Tracing Studies," *Environmental & Engineering Geoscience*, vol. 11, no. 4, pp. 295-308, 2005.
http://eeg.geoscienceworld.org/content/11/4/295.abstract

72. H. C. Hovey, *Mammoth Cave Kentucky Hovey's Practical Guide to the Regulation Routes*, John P. Morton & Company, Inc., Louisville, Kentucky, USA, 1909.

73. LibreOffice Calc (Version 3.5.4.2) [computer software]. (2012). The Document Foundation, retrieved from http://www.libreoffice.org/

74. Solver for Nonlinear Programming/NLPSolver (Version 0.9-beta-1) [computer software]. (2009). Sun Microsystems, Inc., retrieved from

http://extensions.services.openoffice.org/en/project/NLPSolver

75. Apache OpenOffice.org, “NLPSolver” [online] Available: http://wiki.services.openoffice.org/wiki/NLPSolver, (Date- July 10, 2012)

76. C. J. Willmott, K. Matsuura, and S. M. Robeson, “Ambiguities inherent in sums-of-squares-based error statistics,” *Atmospheric Environment*, vol. 43, no. 3, pp. 749-752, 2009. http://www.sciencedirect.com/science/article/pii/S1352231008009564

77. S. C. Chapra, *Applied Numerical Methods with MATLAB for Engineers and Scientists*, 2nd Edition, The McGraw-Hill Companies, Inc., New York, New York, USA, 2008.

78. J. W. Eaton and others, GNU Octave (Version 3.6.1) [computer software]. (2012). Retrieved from http://www.octave.org

79. B. Spitzak and others, FLTK (Version 1.3) [computer software]. (2011). Retrieved from http://www.fltk.org/index.php

80. T. Williams, C. Kelley, and others, gnuplot (Version 4.4.4) [computer software]. (2011). Retrieved from http://www.gnuplot.info

APPENDICES

APPENDIX A

RAW QUANTITATIVE TRACER STUDY DATA

Table A.1 Raw YSI datasonde data for Shaler's Brook

Elapsed Time, min	**Rhodamine [C(t)], µg/L**
0	0
20	0
40	0
60	9269
80	10264
100	9400
120	6814
140	4996
160	3703
180	2774
200	2099
220	1604
240	1237
260	963
280	756
300	599
320	499.8
340	476.7
360	451
380	430.4
400	408.2
420	387.8
440	371.9

Table A.1 Raw YSI datasonde data for Shaler's Brook

Elapsed Time, min	**Rhodamine [C(t)], µg/L**
460	354.1
480	338.5
500	325.6

Table A.2 Raw GGUN-FL Fluorometer 80526 data for Devil's Cooling Tub (1st Hit)

Time, min	**Elapsed Time, min**	**Rhodamine [C(t)], µg/L**
0	47609	0.03
5	47614	0.03
10	47619	0.03
15	47624	0.03
20	47629	0.03
25	47634	0.03
30	47639	0.03
35	47644	0.03
40	47649	0.53
45	47654	1.59
50	47659	1.39
55	47664	1.64
60	47669	1.54
65	47674	1.69
70	47679	82.32
75	47684	1.46
80	47689	1.5
85	47694	6.94
90	47699	439.18
95	47704	1.33
100	47709	1.13
105	47714	818.49
110	47719	17.74
115	47724	105.43
120	47729	1549.27

Table A.2 Raw GGUN-FL Fluorometer 80526 data for Devil's Cooling Tub (1st Hit)

Time, min	Elapsed Time, min	Rhodamine [C(t)], µg/L
125	47734	4.88
130	47739	99.39
135	47744	46.7
140	47749	693.54
145	47754	62.36
150	47759	45.72
155	47764	63.97
160	47769	2.73
165	47774	176.25
170	47779	298.96
175	47784	6.22
180	47789	1302.71
185	47794	210.43
190	47799	284.27
195	47804	77.61
200	47809	198.91
205	47814	236.55
210	47819	25.49
215	47824	312.79
220	47829	188.12
225	47834	461.66
230	47839	0.96
235	47844	1.69
240	47849	22.06
245	47854	1.13

Table A.2 Raw GGUN-FL Fluorometer 80526 data for Devil's Cooling Tub (1st Hit)

Time, min	Elapsed Time, min	Rhodamine [C(t)], µg/L
250	47859	1.05
255	47864	1.19
260	47869	1.18
265	47874	1.11
270	47879	1.1
275	47884	1.01
280	47889	1.16
285	47894	0.97
290	47899	1.08
295	47904	1.15
300	47909	1.12
305	47914	1.01
310	47919	1
315	47924	1.11
320	47929	1.05
325	47934	0.95
330	47939	1.09
335	47944	1.17
340	47949	1.11
345	47954	1.19
350	47959	0.97
355	47964	1.08
360	47969	1.06
365	47974	0.92
370	47979	1.01

Table A.2 Raw GGUN-FL Fluorometer 80526 data for Devil's Cooling Tub (1st Hit)

Time, min	Elapsed Time, min	Rhodamine [C(t)], µg/L
375	47984	0.95
380	47989	0.97
385	47994	0.97
390	47999	0.99
395	48004	0.98
400	48009	1.02
405	48014	0.93
410	48019	0.96
415	48024	0.95
420	48029	0.94
425	48034	0.95
430	48039	0.77
435	48044	0.94
440	48049	0.94
445	48054	0.96
450	48059	0.9
455	48064	0.89
460	48069	0.93
465	48074	0.9
470	48079	0.88
475	48084	0.95
480	48089	0.87

Table A.3 Raw GGUN-FL Fluorometer 80526 data for Devil's Cooling Tub (2nd Hit)

Time, min	**Elapsed Time, min**	**Rhodamine [C(t)], µg/L**
0	52844	0.61
5	52849	0.67
10	52854	0.7
15	52859	146.93
20	52864	188.77
25	52869	86.05
30	52874	118.57
35	52879	226.6
40	52884	1.02
45	52889	2.28
50	52894	2.98
55	52899	101.62
60	52904	20.51
65	52909	92.45
70	52914	2.6
75	52919	555.21
80	52924	488.62
85	52929	1.25
90	52934	0.03
95	52939	41.22
100	52944	170.39
105	52949	1256.58
110	52954	69.94
115	52959	12.59
120	52964	0.03

Table A.3 Raw GGUN-FL Fluorometer 80526 data for Devil's Cooling Tub (2nd Hit)

Time, min	Elapsed Time, min	Rhodamine [C(t)], µg/L
125	52969	573.71
130	52974	17.69
135	52979	344.66
140	52984	27.18
145	52989	82.62
150	52994	231.22
155	52999	1.83
160	53004	36.48
165	53009	203.7
170	53014	1.37
175	53019	1332.92
180	53024	2354.9
185	53029	15.95
190	53034	78.83
195	53039	570.44
200	53044	51.88
205	53049	185.98
210	53054	11.11
215	53059	0.03
220	53064	42.9
225	53069	6.44
230	53074	407.71
235	53079	180.51
240	53084	446.51
245	53089	1639.08

Table A.3 Raw GGUN-FL Fluorometer 80526 data for Devil's Cooling Tub (2nd Hit)

Time, min	**Elapsed Time, min**	**Rhodamine [C(t)], µg/L**
250	53094	57.46
255	53099	28.57
260	53104	203.5
265	53109	313.51
270	53114	882.36
275	53119	29.62
280	53124	20.41
285	53129	665.59
290	53134	597.64
295	53139	130.32
300	53144	1.26
305	53149	946.69
310	53154	202.87
315	53159	1.23
320	53164	1.29
325	53169	1.14
330	53174	1.18
335	53179	1.08
340	53184	1.18
345	53189	1.14
350	53194	1.1
355	53199	1.08
360	53204	1.09
365	53209	0.92
370	53214	0.97

Table A.3 Raw GGUN-FL Fluorometer 80526 data for Devil's Cooling Tub (2nd Hit)

Time, min	Elapsed Time, min	Rhodamine [C(t)], µg/L
375	53219	1.03
380	53224	1.04
385	53229	0.97
390	53234	0.97
395	53239	1.06
400	53244	1.04
405	53249	0.98
410	53254	1.09
415	53259	1.02
420	53264	1.08
425	53269	1.03
430	53274	0.96
435	53279	1.04
440	53284	0.99
445	53289	0.99
450	53294	1.05
455	53299	1.03
460	53304	0.9
465	53309	0.91
470	53314	1.05
475	53319	0.99
480	53324	1.07

APPENDIX B

COMPUTER PROGRAM

saved as runsite.m

```
tspan_min = csvread(“Gamma-ADE-Tracer-Transform.csv”, ‘A7..A32’);
tspan_dimless = csvread(“Gamma-ADE-Tracer-Transform.csv”, ‘B8..B32’);
alpha1 = csvread("Gamma-ADE-Tracer-Transform.csv", 'B2..B2');
alpha2 = csvread("Gamma-ADE-Tracer-Transform.csv", 'B3..B3');
beta1 = csvread("Gamma-ADE-Tracer-Transform.csv", 'C2..C2');
beta2 = csvread("Gamma-ADE-Tracer-Transform.csv", 'C3..C3');
[tspan_min, tspan_dimless, restime_dimless] =
rtimeGNUOctave(alpha1,alpha2,beta1,beta2,tspan_min,tspan_dimless);
```

saved as rtimeGNUOctave.m

```
function [tspan_min, tspan_dimless, restime_dimless] =
rtimeGNUOctave(alpha1,alpha2,beta1,beta2,tspan_min,tspan_dimless)

#{
rtimeGNUOctave: Residence Time Distribution (RTD) function analytical
function written specifically for GNU Octave
Author: Irucka Embry
Copyright (C) 2011, 2012 by Irucka Ajani Embry
This function is free software; you can redistribute it and/or modify it
under the terms of the GNU General Public License as published by the
Free Software Foundation; either version 2 of the License, or (at your
option) any later version.
This function rtimeGNUOctave is distributed in the hope that it will be
useful, but WITHOUT ANY WARRANTY; without even the implied warranty of
MERCHANTABILITY or FITNESS FOR A PARTICULAR PURPOSE. See the GNU General
Public License for more details.
The GNU General Public License can be viewed online at
<http://www.gnu.org/licenses/>.
[tspan_min, tspan_dimless, restime_dimless] =
rtimeGNUOctave(alpha1,alpha2,beta1,beta2,tspan_min,tspan_dimless):
This function compares the normalized forms of the advection dispersion
equation (ADE), tracer, and the gamma distribution RTD models computed
from a quantitative dye tracer study.
 input:
    alpha1 = shape parameter in the gamma RTD model
    alpha2 = shape parameter in the gamma RTD model
    beta1 = scale parameter in the gamma RTD model
    beta2 = scale parameter in the gamma RTD model
    tspan_min = elapsed time used to produce the tracer breakthrough
```

```
curve
    tspan_dimless = elapsed normalized time used to produce the
normalized RTD curve
 output:
    restime_dimless = the gamma distribution probability density function
(PDF) of the residence time, otherwise known as the gamma distribution
residence time distribution function E(t)
    tm = mean residence time for the non-ideal flow system or the mean
time in the system
    sigmasqr = variance (measure of the distribution width)
    mean_distance_traveled = mean travel distance of the tracer molecules
    mean_velocity = mean travel distance of tracer molecule/mean time in
the system
    MADg = mean-absolute deviation of the gamma RTD model from the tracer
RTD model (normalized forms)
    MADa = mean-absolute deviation of the advection dispersion equation
RTD model from the tracer RTD model (normalized forms)
#}

if nargin<4,error('at least 6 input arguments required'),endif
if any(diff(tspan_min)<=0),error('tspan not ascending order'),endif
if any(diff(tspan_dimless)<=0),error('tspan not ascending order'),endif
if alpha1<1,error('alpha1 must be greater than or equal to 1'),endif
if alpha2<1,error('alpha2 must be greater than or equal to 1'),endif
if beta1<0,error('beta1 must be greater than or equal to 0'),endif
if beta2<0,error('beta2 must be greater than or equal to 0'),endif

format short g;

conc = csvread("Gamma-ADE-Tracer-Transform.csv", 'C7..C32');
conc = conc(:); %convert to column vector

ADE_dimless = csvread("Gamma-ADE-Tracer-Transform.csv", 'V8..V32');
ADE_dimless = ADE_dimless(:); %convert to column vector

Tracer_dimless = csvread("Gamma-ADE-Tracer-Transform.csv", 'N8..N32');
Tracer_dimless = Tracer_dimless(:); %convert to column vector

%for normalized time
n = length(tspan_dimless);
tspan_dimless = tspan_dimless(:); %convert to column vector
ti = tspan_dimless(1); tf = tspan_dimless(n);
if n == 2
  t = (ti:h:tf)'; n = length(t);
  if t(n) < tf
    t(n+1) = tf;
    n = n+1;
```

```
  endif
else
t = tspan_dimless;
endif

restime_dimless = (gamma(alpha1+alpha2)/
(gamma(alpha1)*gamma(alpha2)))*((beta1/beta2)^(alpha2))*((t.^(alpha1-1)).
/((t.+(beta1/beta2)).^(alpha1+alpha2)));
m = length(restime_dimless);
m = n;
restime_dimless = restime_dimless(:); %convert to column vector
%if length(m)~=n, error('n and m must be the same length'); endif

tm = (beta1/beta2)*(alpha1/(alpha2-1)); %tm = mean residence time for the
non ideal flow system

sigmasqr = ((beta1/beta2)^2)*(alpha1/(alpha2-1))*((alpha1+1)/
(alpha2-2)-(alpha1/(alpha2-1))); %sigmasqr = variance (measure of the
distribution width)

mean_distance_traveled = alpha1*beta1;

mean_velocity = (alpha2-1)*beta2;

n = length(tspan_dimless);

MADg = n^-1 * sum(abs(restime_dimless - Tracer_dimless));

MADa = n^-1 * sum(abs(ADE_dimless - Tracer_dimless));

close all; %closes all open figures; Source: "Plotting in Matlab - A
quick tutorial" by Peter Norgaard
graphics_toolkit gnuplot
figure; %opens a new figure; Source: "Plotting in Matlab - A quick
tutorial" by Peter Norgaard
plot (tspan_min, conc, "b", 'linewidth', 2);
ax = gca();
set(ax, 'fontsize', 14);
grid("off");
axis("tight");
title('Tracer Breakthrough Curve for Site');
xlabel('Time (minutes)');
ylabel('Dye Concentration (\mug/L)');
print -textspecial figure-conc-gnuplot.png
print -textspecial figure-conc-gnuplot.svg

graphics_toolkit gnuplot
```

```
figure; %opens a new figure; Source: "Plotting in Matlab - A quick
tutorial" by Peter Norgaard
plot (tspan_dimless, restime_dimless, "b", 'linewidth', 2, tspan_dimless,
Tracer_dimless, "r", 'linewidth', 2, tspan_dimless, ADE_dimless, "g",
'linewidth', 2);
ax = gca();
set(ax, 'fontsize', 14);
grid("off");
axis("tight");
title('Normalized RTD Models for Site');
xlabel('Normalized Time');
ylabel('Normalized RTD');
legend({"Gamma RTD", "Tracer RTD", "ADE RTD"}, "location", "northeast");
%http://octave.sourceforge.net/octave/function/legend.html
print -textspecial figure-RTD-norm-gnuplot.png
print -textspecial figure-RTD-norm-gnuplot.svg

save rtimeGNUOctaveResults.txt restime_dimless mean_distance_traveled
mean_velocity tm sigmasqr MADg MADa
endfunction
```

Irucka Embry, E.I.T.
1516A Lillian Street | Nashville, TN 37206 | (615) 713-7094 |
iruckaE@mail2world.com

Education:
Master of Engineering, Tennessee State University (August 2012)
Concentration in Environmental Engineering
Overall Cumulative GPA: 4.00/4.00

Post-Baccalaureate Program, University of Kentucky
Civil and Environmental Engineering
Overall Cumulative GPA: 3.58/4.00

BS in Civil Engineering, University of Tennessee (August 2004)
Concentration in Environmental Engineering
Minor in Spanish

Professional Certification:
Engineer-in-Training (E.I.T.) certified by the Tennessee Board of Architectural and Engineering Examiners
Registered on June 3, 2004

Publications:
I. Embry, V. Roland, R. Painter, R. Toomey, and L. Sharpe, "Quantitative dye tracing – development of a new interpretative method," *Proceedings of the 22nd Tennessee American Water Resources Association (AWRA) Tennessee Water Resources Symposium*, Burns, Tennessee, USA, pp. 1C-6--1C-16, 2012.

R. Diehl, R. Toomey, V. Roland, I. Embry, A. West, "Effectiveness of Stormwater Filters at Mammoth Cave National Park, Kentucky," *Proceedings of the 22nd Tennessee American Water Resources Association (AWRA) Tennessee Water Resources Symposium*, Burns, Tennessee, USA, pp. P-29--P-36, 2012.

I. Embry, R. Painter, T. D. Byl, "Residence Time Distribution Model for Non-ideal Flow Derived from Independent Gamma Distributions of Tracer Travel Distance and Linear Velocity," Abstract Book of the 32nd Annual Meeting in North America of the Society of Environmental Toxicology and Chemistry (SETAC), Boston, Massachusetts, USA, pp. 198--198, 2011.

I. Embry and R. Painter, "Graphical Residence Time Distribution Model for Karst Systems

Using MATLAB® and GNU Octave Derived from Independent Gamma Distributions of Tracer Travel Distance and Linear Velocity," *Proceedings of the 21st Tennessee American Water Resources Association (AWRA) Tennessee Water Resources Symposium*, Burns, Tennessee, USA, pp. P-22--P-22, 2011.

I. Embry, "Social Sustainability and the Pursuit of Design in Engineering," EWRI [Environmental & Water Resources Institute of the American Society of Civil Engineers (ASCE)] *Environmental and Water Engineering Practice*, vol. 1, no. 1, pp. 5, 2011.

H. Hilger and I. Embry, "Towards a New Vision of Social Sustainability," EWRI *Currents*, vol. 12, no. 4, pp. 10-11, 2010.

Research Symposium Poster Presentation:
I. Embry, R. Painter, T. D. Byl, "Residence Time Distribution Model for Non-ideal Flow Derived from Independent Gamma Distributions of Tracer Travel Distance and Linear Velocity." Presented at the 34th Annual Tennessee State University-Wide Research Symposium in Nashville, Tennessee, on March 29, 2012.

Experience:
Physical Science Technician, May 2012 – Present & August 2011 – September 2011
U. S. Geological Survey (USGS) Tennessee Water Science Center
Nashville, TN

- Working on surface water nutrient modeling projects.
- Performed groundwater laboratory analysis for both the Hardeman County Landfill (Tennessee) and Mammoth Cave National Park (Kentucky).

Graduate Student Researcher, January 2011 – Present
Tennessee State University Civil and Environmental Engineering Department
Nashville, TN

- Researching the fate and transport mechanisms of contaminants in karst aquifer systems.

Principal, November 2007 – Present
2
EcoC S
Nashville, TN

- Used various teaching strategies to help students better understand Beginner through Intermediate Spanish, General College Chemistry, Algebra 1, Geometry, and High School Physics.